AN ABSTRACT OF THE THESIS OF

Richard M. Williams, Jr. (Name) for the degree Doctor of Philosophy (Degree)

in Oceanography (Major) presented on January 11, 1974 (Date)

Title: HIGH FREQUENCY TEMPERATURE AND VELOCITY FLUCTUATIONS IN THE ATMOSPHERIC BOUNDARY LAYER

Abstract approved: Redacted for privacy

Dr. Clayton A. Paulson

Turbulent temperature and velocity fluctuations in air were measured over an open field during the summer at a height of 2 meters. Emphasis was placed on precisely determining the high frequency region of the spectra of these fluctuations, including the dissipation range. The velocity fluctuations were measured with a commercially available hot-wire anemometer, with a wire diameter of 3.7 μ and length approximately 1 mm. The temperature fluctuation measurements were made with a platinum resistance thermometer which consisted of a platinum wire of 0.5 μ diameter and about 1 mm in length. The temperature measuring system was developed as part of the research.

The velocity spectra results agree well with previous results of Pond, et al. (1963), Nasmyth (1970) and Boston (1970). The estimated value of the one-dimensional Kolmogorov constant, α, was 0.50 in

agreement with Boston but 10% lower than the value of Nasmyth.

The results of the temperature spectra show clearly the shape of the one-dimensional temperature well beyond the -5/3 region. The temperature spectrum has its maximum dissipation at higher frequency than does the velocity spectrum. An unexpected result is an increase in slope of the temperature spectrum (greater than -5/3) at frequencies just below the frequency of maximum dissipation. Calculation was made of the one-dimensional Kolmogorov constant for temperature, β, by directly measuring all parameters required. The estimated value is 1.02, which may be compared to 1.6 and 2.3 reported by Boston (1970) and Gibson, et al. (1970) respectively.

Fluxes of momentum and sensible heat were computed for 13 runs under both stable and unstable conditions. Two techniques used for these flux determinations were the direct or eddy correlation method and the dissipation method. Stress estimated by the dissipation method exceeded estimation by the direct method by about 10%. In general excellent agreement was found in the sensible heat flux estimates.

High Frequency Temperature and Velocity Fluctuations in the Atmospheric Boundary Layer

by

Richard Melton Williams, Jr.

A THESIS

submitted to

Oregon State University

in partial fulfillment of
the requirements for the
degree of

Doctor of Philosophy

Completed January 1974

Commencement June 1974

APPROVED:

Redacted for privacy

Associate Professor of Oceanography

in charge of major

Redacted for privacy

Dean of School of Oceanography

Redacted for privacy

Dean of Graduate School

Date thesis is presented January 11, 1974

Typed by Clover Redfern for Richard M. Williams, Jr.

ACKNOWLEDGMENT

I would like to thank my supervisor, Dr. C. A. Paulson, for providing encouragement and insight into the many problems encountered. Mr. Leon Childears of the Oceanography Department performed much of the mechanical work involved in the field experiment. Special thanks goes to Mr. Laudie Doubrava for his invaluable assistance in the design and assembly of the temperature sensor electronics. Mr. Jaffer Raza and Mr. James Simpson were responsible for improving the existing analog-to-digital converter so that the required higher digitization rates could be handled. Many other people contributed ideas and assistance to me while my work was in progress, among them are my fellow students in the air-sea interaction group, members of my doctoral committee and my family.

My studies toward a Ph. D. were supported by the Office of Naval Research under contract N00014-67-A-0369-0007.

TABLE OF CONTENTS

LIST OF FIGURES

LIST OF TABLES

HIGH FREQUENCY TEMPERATURE AND VELOCITY FLUCTUATIONS IN THE ATMOSPHERIC BOUNDARY LAYER

I. INTRODUCTION

Over the past several years various attempts have been made to measure small scale temperature fluctuations in the atmospheric boundary layer. These data were then used to determine the "universal" constant, β, appearing in the expression for the -5/3 form of the temperature spectrum. β is called the Kolmogorov scalar constant after A.N. Kolmogorov (1941), who postulated a similar constant for velocity spectra. In order to directly measure the scalar constant, a direct measure of the dissipation of temperature and velocity variance is required. To achieve this goal the sensors must have sufficiently high frequency response and small spatial resolution to measure the small scale fluctuations associated with the dissipation of temperature and velocity fluctuations. In addition to sensor requirements, the associated electronics must be of very low noise design while maintaining adequate frequency response.

The object of the first stage of research was to develop the required sensor and sensor electronics. Subsequent to this stage a field experiment was conducted in which the small scale fluctuations of temperature and velocity were measured over homogeneous terrain. Data analysis yielded the shape of the temperature spectrum and an

evaluation of the constant, β.

Knowledge of the value of the Kolmogorov constants for velocity and temperature are required for use of the dissipation method in determining the fluxes of momentum and sensible heat. Direct measurement of these fluxes is given by the covariances of the horizontal and vertical velocity fluctuations and of the vertical velocity and temperature fluctuations. However, this method requires rather sophisticated instrumentation for measuring the components of the velocity. Such instrumentation would be nearly useless for shipboard measurements where ship motion would contaminate the data. A much simpler procedure would involve measurement of the spectra of the horizontal velocity component and temperature in the -5/3 range. From these spectral estimates the rates of dissipation of kinetic energy and temperature variance could be determined, provided the values of the Kolmogorov constants are known. The rates of dissipation then determine the fluxes in the dissipation method. One of the research objectives was to compare these fluxes determined by both techniques.

II. THEORETICAL CONSIDERATIONS

A. General Considerations

Turbulent flow may be described as random motions of a fluid which cannot be uniquely determined by the macroscopic parameters of the flow (Batchelor, 1953). Due to this randomness a statistical description is used. Basic to any statistical description is the average. In principle an average over an infinite collection of identical conditions is desired. Such an average is referred to as an ensemble average. However, in practice a space or time average is obtained. Under the condition that the turbulence is stationary a space or time average is equivalent to an ensemble average. This equivalence is referred to as the ergodic hypothesis (Tennekes and Lumley, 1972).

All flow variables are assumed to be composed of mean and fluctuating parts. The notation used in this thesis will be that mean quantities will have an overbar and fluctuating quantities will be lower case. For motions near a horizontal boundary the mean velocity in the vertical direction will be assumed to be zero. Thus the velocity and temperature are represented by:

$$\begin{aligned} U &= \overline{U} + u \\ W &= \overline{W} + w = w \\ T &= \overline{T} + \theta \end{aligned} \tag{1-1}$$

where:

U is the downstream velocity

W is the vertical velocity

T is the temperature

Extensive use is made of spectral analysis in this research. The spectrum of a variable, x, is the distribution of the variance of x as a function of the scale size or frequency of the fluctuations of x. This is formalized in the following definition.

$$S_x(\omega) = \frac{\overline{x^2}}{\pi} \int_{-\infty}^{\infty} e^{-i\omega\tau} \rho_x(\tau) d\tau \qquad (1\text{-}2)$$

where:

$S_x(\omega)$ = spectral density of x

ω = radian frequency

$\rho(\tau)$ = autocorrelation function of x

τ = time lag

Since $S_x(\omega)$ represents the frequency distribution of the variance of x, integration over all frequencies will yield the total variance of x.

$$\overline{x^2} = \int_0^{\infty} S_x(\omega) d\omega \qquad (1\text{-}3)$$

One of the properties of turbulent flow is that mechanical energy is transferred to internal energy. This is referred to as dissipation.

In addition, the turbulent fluctuation of temperature is dissipated through the action of thermal diffusion. The primary objective of this research is to directly measure the rate of dissipation for both turbulent temperature and velocity fluctuations.

All experimental measurements were made as a time series at a fixed location in the flow field. Subsequent spectral calculations were made in terms of frequency. Time and space scales were then related by Taylor's "Frozen Turbulence" hypothesis (Taylor, 1938),

$$x = \overline{U}t \tag{1-4}$$

where $\overline{U}$ is the mean wind speed. This relation implies that the turbulence is unchanged during the time required for it to pass the sensors. Equivalently the radian wavenumber, k, circular frequency, f, and radian frequency, ω, are related by:

$$k = 2\pi f/\overline{U} = \omega/\overline{U} \tag{1-5}$$

For shear flow this relation cannot be rigorously justified (Lumley, 1965) but it may still be valid for low turbulence intensity $\sqrt{\overline{u^2}}/\overline{U}$ and for wavenumbers which satisfy

$$kz \gg 1 \tag{1-6}$$

where z is the distance from the boundary. This condition is satisfied for those wavenumbers contributing to the dissipation.

Another transformation important to this thesis is the spectral transformation between a variable and its time derivative. The correlation function, $\rho_x(\tau)$ and the spectral density, $S(\omega)$, are related by:

$$\rho_x(\tau) = \frac{1}{\overline{x^2}} \int_{-\infty}^{\infty} e^{i\omega\tau} S_x(\omega) d\omega \tag{1-7}$$

and

$$\rho_{x'}(\tau) = \frac{1}{\overline{x'^2}} \int_{-\infty}^{\infty} e^{i\omega\tau} S_{x'}(\omega) d\omega \tag{1-8}$$

where:

$$x' = \frac{\partial x}{\partial t}$$

The correlation function is defined by:

$$\rho_x(\tau) = \overline{x(t)x(t+\tau)}/\overline{x^2} \tag{1-9}$$

and

$$\rho_{x'}(\tau) = \overline{x'(t)x'(t+\tau)}/\overline{x'^2} \tag{1-10}$$

letting $t + \tau = t'$ and differentiating Eqn. (1-9) with respect to t and t' gives:

$$\frac{\partial^2 \rho_x(\tau)}{\partial t \partial t'} = \frac{\overline{x'(t)x'(t')}}{\overline{x^2}} \tag{1-11}$$

or

$$\frac{\partial^2 \rho_x(\tau)}{\partial \tau^2} = -\frac{\overline{x'(t)x'(t+\tau)}}{\overline{x^2}} \tag{1-12}$$

Substituting Eqn. (1-12) into Eqn. (1-10) gives:

$$\rho_{x'}(\tau) = \frac{\overline{x^2}}{\overline{x'^2}} \frac{\partial^2 \rho_x(\tau)}{\partial \tau^2} \tag{1-13}$$

An expression for $\frac{\partial^2 \rho_x(\tau)}{\partial \tau^2}$ can be obtained by twice differentiating Eqn. (1-7).

$$\frac{\partial^2 \rho_x(\tau)}{\partial \tau^2} = -\frac{1}{\overline{x^2}} \int_{-\infty}^{\infty} e^{i\omega\tau} \omega^2 S_x(\omega) d\omega \tag{1-14}$$

Now using Eqns. (1-8) and (1-13) gives:

$$S_{x'}(\omega) = \omega^2 S_x(\omega) \tag{1-15}$$

Alternate expressions are of course available as functions of circular frequency, f, and radian wavenumber, k.

$$S_{x'}(k) = (\overline{U})^2 k^2 S_x(k) \tag{1-16}$$

and

$$S_{x'}(f) = (2\pi)^2 f^2 S_x(f) \tag{1-17}$$

B. Universal Spectral Forms

1. Kolmogorov Hypotheses

Development of modern turbulence theories began in 1935 with the concept of a continuous cascade of kinetic energy from large scale anisotropic velocity fluctuations to smaller, and increasingly isotropic, scales at which the energy is dissipated as heat (Taylor, 1935). As the scales separate, the fine structure of the velocity field is hypothesized to become increasingly independent of the directional details of the large scale features. This idea was first mathematically formulated by Kolmogorov (1941). Application of the Kolmogorov hypotheses is warranted provided only that the Reynolds number, Re, is sufficiently large to guarantee a large scale size separation between the energy containing turbulent motions and the viscous dissipative motions.

The Kolmogorov theory proposes that at some point in the small scale region of the energy cascade the turbulent motion becomes isotropic. This is referred to as local isotropy since the large scale motions may not be isotropic. The Kolmogorov ideas are contained in two universal similarity hypotheses:

1) At sufficiently high Re there exists a range of small scales such that the turbulence is statistically in equilibrium and uniquely determined by the mean rate of kinetic energy

dissipation, ϵ, and the kinematic viscosity, ν, (i.e., $S(k) = F(\epsilon, \nu, k)$, Hinze (1959). Dimensional arguments lead to the following universal spectral form:

$$S_u(k) = \epsilon^{1/4} \nu^{5/4} F(k/k_s) \tag{1-18}$$

where: k_s = Kolmogorov wavenumber

$= (\epsilon/\nu^3)^{1/4}$

$F(k/k_s)$ = universal spectral function for velocity.

2) At very large Re the spectrum is independent of ν and depends solely on ϵ in the region of scale sizes far above the region of maximum dissipation but still within the locally isotropic range. Here dissipation will be small compared to energy transfer by inertial effects. This range is thus named the inertial subrange. Dimensional arguments result in the following spectral form.

$$S_u(k) = \alpha \epsilon^{2/3} k^{-5/3} \tag{1-19}$$

where: α = Kolmogorov universal constant.

Using similar arguments Obukhov (1949) and Corrsin (1951) independently arrived at spectral forms for turbulent scalar fluctuations. For scalars an additional parameter is required in the parameterization. This is the mean rate of dissipation of scalar

fluctuations, ϵ_T (using temperature as the scalar). The universal spectral form for temperature is:

$$S_T(k) = \epsilon_T \epsilon^{-3/4} \nu^{5/4} H(\sigma, k/k_s) \tag{1-20}$$

where:

σ = Prandtl number

$H(\sigma, k/k_s)$ = Universal spectral function for temperature

In the inertial subrange this form becomes:

$$S_T(k) = \beta \epsilon^{-1/3} \epsilon_T k^{-5/3} \tag{1-21}$$

An additional constraint on the application of similarity hypotheses to scalar fields is that they are assumed to be dynamically passive. A passive scalar is one that can be transported in a fluid but which does not introduce buoyance effects. The scalar fluctuations of temperature are active at large scales but not at the small scales important to the results of this thesis.

2. Observations

Numerous results concerning the Kolmogorov hypotheses are available. The results of Grant, et al. (1962) from velocity measurements in a tidal channel and of Pond, et al. (1963) working in the atmosphere bear out the validity of a universal spectral form.

Additionally the -5/3 power dependence of the wavenumber is verified. Further support is obtained from verification of the expected ratio of the spectra of the lateral and vertical velocity components to the spectra of downstream components under locally isotropic conditions. Kaimal, et al. (1972) found the expected 4/3 ratio at wavelengths of the order of the measurement height, z. Accordingly, the Kolmogorov constant α of Eqn. (1-19) should be absolute, independent of the fluid or of the nature of the mean flow. Pond, et al. (1966) summarized the measured values of α from various different flow fields. The mean value of α was 0.48. More recent investigations by Shieh, et al. (1971), Gibson, et al. (1970), and Nasmyth (1970) have yielded larger values. A reasonable average now appears to be, $\alpha = 0.55$.

Results for scalar variables are less numerous but enough exist to verify the validity of the scalar Kolmogorov forms. Grant, et al. (1968) obtained temperature fluctuations in the ocean and show a well defined -5/3 region. Gibson, et al. (1970) and Boston (1970) have measured temperature fluctuations in the atmosphere to very high wavenumbers.

The constant β of Eqn. (1-21) is predicted to be an absolute one. Most previous measurements of β have depended on measured scalar spectra which have been poorly defined at high wavenumbers. Indirect measurements of β generally result in estimates between

0.6 and 0.9. Gibson and Schwarz (1963) estimated a value of 0.7 for scalar fluctuations of salinity in a laboratory water tunnel. Grant, et al. (1968) indirectly estimated β to be 0.62 for temperature fluctuation in a tidal channel. Using structure functions, Paquin and Pond (1971) estimated values of 0.83 and 0.80 for temperature and humidity fluctuations. Based on the 1968 AFCRL experiment in Kansas, Kaimal, et al. (1972) estimated β to be 0.83 using an indirect measure of ϵ_T. However, recent determinations by Boston (1970) and Gibson, et al. (1970), using very small sensors to measure directly the dissipation of temperature variance, have yielded values of 1.6 and 2.3 respectively.

Clearly, the constant is not well known. In fact some doubts have arisen as to whether it is a constant at all. Suggestions have been made that both constants α and β may be functions of stability (Boston, 1970). The temperature measurements reported in this thesis were an attempt to resolve some of this uncertainty.

C. Dissipation and Evaluation of Universal Constants

1. Spectral Transformations

Kolmogorov's spectral relations are generally written in terms of radian wavenumber while measurements are generally taken with respect to time with subsequent spectral estimates in terms of

frequency. Using the definitions relating radian and circular frequency and Taylor's hypothesis to relate wavenumber and frequency the relations between the spectral functions are give by:

$$S_x(k) = (\frac{\overline{U}}{2\pi})S_x(f) = \overline{U}S_x(\omega) \qquad (1\text{-}22)$$

These relations are also true for any derivative of x. Additionally we have the relations between the spectra of a variable and its derivative, Eqns. (1-15) to (1-17).

2. Evaluation of Dissipation

a. Velocity. The equation of motion for turbulent flow can be used to generate an energy conservation equation for mechanical energy. There is one term in this expression which represents a sink for mechanical energy by transforming mechanical energy into heat through the action of viscosity. This is called the dissipation term and is given by:

$$\epsilon = \frac{\nu}{2}\overline{(\frac{\partial u_i}{\partial x_j} + \frac{\partial u_j}{\partial x_i})^2} \qquad (1\text{-}23)$$

where: ν = kinematic viscosity (cm^2/sec).

The subscript indices represent the three coordinates and indicates use of the Einstein tensor notation where summation is assumed over

repeated indices. Thus, Eqn. (1-23) consists of 18 separate terms. Fortunately, under conditions of isotropy the terms are all interrelated. These relations are given in Goldstein (1938). The simplified expression for ϵ is:

$$\epsilon = 15\nu\overline{(\frac{\partial u}{\partial x})^2} \tag{1-24}$$

Using Taylor's hypothesis the space derivative can be transformed to a time derivative.

$$\epsilon = 15\nu(\frac{1}{\overline{U}^2})\overline{(\frac{\partial u}{\partial t})^2} \tag{1-25}$$

Now ϵ can be expressed as a function of the spectrum of $\frac{\partial u}{\partial t}$ using the spectral definition given in Eqn. (1-3).

$$\epsilon = 15\nu(\frac{1}{\overline{U}^2})\int_0^\infty S_{u'}(k)dk \tag{1-26}$$

Using Eqn. (1-16) the more familiar expression for dissipation is obtained.

$$\epsilon = 15\nu\int_0^\infty k^2 S_u(k)dk \tag{1-27}$$

The expressions $S_{u'}(k)$ and $k^2 S_u(k)$ are commonly called the dissipation spectra. A better signal-to-noise ratio is obtained by

recording the time derivative signal and thus Eqn. (1-26) should yield a better estimate of the dissipation.

b. Temperature. An equation analogous to the mechanical energy conservation equation can be written for the temperature variance. This expression also has a term which represents a loss of temperature variance and is given by:

$$\epsilon_T = D_T \overline{\left(\frac{\partial \theta}{\partial x_i}\right)^2} \tag{1-28}$$

where: D_T = thermal diffusivity (cm^2/sec).

Isotropy is again assumed to allow simplification of Eqn. (1-28) to:

$$\epsilon_T = 3D_T \overline{\left(\frac{\partial \theta}{\partial x}\right)^2} \tag{1-29}$$

Taylor's hypothesis may be used to convert this to a time derivative.

$$\epsilon_T = 3D_T \left(\frac{1}{\overline{U}^2}\right) \overline{\left(\frac{\partial \theta}{\partial t}\right)^2} \tag{1-30}$$

Using the spectral definition this becomes,

$$\epsilon_T = 3D_T \left(\frac{1}{\overline{U}^2}\right) \int_0^\infty S_{T'}(k)dk \tag{1-31}$$

This can also be converted to the more familiar form:

$$\epsilon_T = 3D_T \int_0^\infty k^2 S_T(k)dk \qquad (1\text{-}32)$$

The principal problem with measuring the thermal dissipation by this method in the past was due to poor signal-to-noise characteristics of the sensor electronics. One of the primary results shown in this thesis is the development of temperature sensor electronics permitting the entire dissipation spectrum to be measured with negligible noise effects.

3. Evaluation of Kolmogorov Universal Constants

Once the spectrum and dissipation are measured it is a simple matter to calculate the Kolmogorov constants using Eqns. (1-19) and (1-21). Thus,

$$\alpha = S_u(k)\epsilon^{-2/3}k^{5/3} \qquad (1\text{-}33)$$

or using the velocity derivative signal,

$$\alpha = S_{u'}(k)\left(\frac{1}{\overline{U}^2}\right)\epsilon^{-2/3}k^{-1/3} \qquad (1\text{-}34)$$

The constant for temperature is given by

$$\beta = S_T(k)\epsilon^{1/3}\epsilon_T^{-1}k^{5/3} \qquad (1\text{-}35)$$

or using the temperature derivative signal,

$$\beta = S_{T'}(k)\left(\frac{1}{\overline{U}^2}\right)\epsilon^{1/3}\epsilon_T^{-1}k^{-1/3} \qquad (1\text{-}36)$$

Thus the procedure for evaluation of the universal constants is to directly measure the mean rate of dissipation by integrating the spectrum over all wavenumbers and then to use spectral estimates within the intertial subrange to compute the constants.

D. Flux Determination

In addition to the primary research objective, the fluxes of momentum and sensible heat were measured by two methods. These methods are the eddy-correlation and dissipation techniques.

1. Eddy-Correlation Method

This technique is a direct measure of the fluxes. However, fairly sophisticated instrumentation is required to measure the horizontal and vertical velocity components of the flow. By definition and momentum flux (stress) and sensible heat flux are given by:

$$\tau = -\rho\overline{uw} \qquad (1\text{-}37)$$

and

$$H_s = -\rho c_p\overline{w\theta} \qquad (1\text{-}38)$$

where:

ρ = air density (gm/cm^3)

c_p = specific heat at constant pressure ($cal/gm-°C$)

$\overline{uw}$ = covariance between u and w

$\overline{w\theta}$ = covariance between w and θ

The covariances required can be determined by integrating the cospectra of u-w and w-θ.

$$\overline{uw} = \int_0^\infty Co_{uw}(k)dk \tag{1-39}$$

$$\overline{w\theta} = \int_0^\infty Co_{w\theta}(k)dk \tag{1-40}$$

2. Dissipation Method

The basis of the dissipation method of flux evaluation is to use the simplified conservation equation for mechanical energy and thermal variance. The equations are simplified by assuming that the transfer terms are negligible. McBean, et al. (1971), have examined the turbulent energy budget and found this assumption to be valid for slightly unstable conditions. For stable or neutral conditions the turbulence showed considerable anisotropy so that the dissipation could not be determined. For more unstable conditions the dissipation exceeded production.

Based on the AFCRL experiment in Kansas, Wyngaard and Coté (1971) examined the budgets of both turbulent kinetic energy and temperature variance. Under stable conditions the assumption that production equals dissipation is verified. Under unstable conditions the buoyant production must be included and divergence of vertical transport becomes more important for increasing instability. The temperature variance budget is well approximated by a balance between production and dissipation with only about 10% contribution from divergence of vertical turbulent transport.

The simplified equations are given by:

$$\overline{uw}\frac{\partial \overline{U}}{\partial z} - \frac{g}{\overline{T}}\overline{w\theta} = -\epsilon \tag{1-41}$$

$$\overline{w\theta}\frac{\partial \overline{T}}{\partial z} = -\epsilon_T \tag{1-42}$$

Using Monin-Oboukhov similarity theory (1954) the budget equation can be used to obtain estimates of stress and heat flux. First the following scaling parameters are defined.

$$u_* = \text{"friction velocity"} \tag{1-43}$$

$$= \sqrt{\tau/\rho}$$

$$\theta_* = \text{temperature scale}$$

$$= -H_s/\kappa\rho c_p u_*$$

where: κ = VonKarman's constant = 0.4.

Use of dimensional analysis predicts the form of the mean velocity and temperature gradients.

$$\frac{\partial \bar{U}}{\partial z} = \frac{u_*}{\kappa z} F_1(z/L) \tag{1-44}$$

$$\frac{\partial \bar{T}}{\partial z} = \frac{\theta_*}{z} F_2(z/L) \tag{1-45}$$

Where $F(z/L)$ is a nondimensional gradient which is a function only of the non-dimensional stability parameter, z/L. The length scale L is called the Monin-Oboukhov length and is defined by:

$$L = -\frac{u_*^3 \rho c_p \bar{T}}{\kappa g H_s} = \frac{u_*^2 \bar{T}}{g \kappa^2 \theta_*} \tag{1-46}$$

Combining the similarity relation with the budget equations results in the following modified budget equations.

$$-\frac{u_*^3}{\kappa z} F_1(z/L) + \frac{g \kappa u_* \theta_*}{\bar{T}} = -\epsilon \tag{1-47}$$

$$-\frac{\kappa u_* \theta_*^2}{z} F_2(z/L) = -\epsilon_T \tag{1-48}$$

The forms of the non-dimensional gradients have been determined experimentally by numerous investigators. The following

expressions are generally accepted (Lumley and Panofsky, 1964).

for $z/L < 0.0$ (unstable)

$$F_1 = (1-16\ z/L)^{-1/4} \tag{1-49}$$

$$F_2 = (1-16\ z/L)^{-1/2} \tag{1-50}$$

for $z/L > 0.0$ (stable

$$F_1 = F_2 = (1+7\ z/L) \tag{1-51}$$

The solution of Eqns. (1-47) and (1-48) are:

$$u_* = [((\frac{g\kappa z}{\overline{T}})\kappa u_* \theta_* + \epsilon\kappa z)/F_1]^{1/3} \tag{1-52}$$

$$\theta_* = (\epsilon_T z/\kappa u_* F_2)^{1/2} \tag{1-53}$$

An iterative technique is used to solve for u_*, θ_* and z/L, with subsequent transformation to obtain the momentum and sensible heat fluxes. Note that the only parameters required are the mean rates of dissipation for velocity and temperature fluctuations, the measurement height and the mean temperature.

III. EXPERIMENTAL APPROACH

There were two primary developmental efforts required to fulfill the research goals. The most important of these was the development of a temperature measuring system to meet the demanding requirements of a direct measure of the dissipation of temperature fluctuations. These requirements included high frequency response, small sensor size, low velocity sensitivity and very low noise. The other electronic development was of a low noise differentiator for the temperature and velocity signals. The motivation for differentiating these signals was to achieve a higher signal to noise ratio for recording the high frequency fluctuations of interest. Another way of viewing differentiation is that it acts to prewhiten the spectra of these signals.

Of equal importance to suitable temperature measurement is the velocity measurement since the mechanical dissipation, as well as the thermal dissipation, is required for calculation of the Kolmogorov constant for temperature. Fortunately excellent commercial systems are available in the form of hot-wire anemometers.

The following sections will discuss the specific sensor requirements, the electronics development, secondary instrumentation used, and data acquisition system.

A. Sensor Requirements and Selection

1. Temperature

The severe requirements limited the available techniques to just one, resistance thermometry. This technique uses a small wire, with a high temperature coefficient of resistance, as a sensor. Changes in resistance (i.e. temperature) are detected as changes in voltage drop across the wire when a low constant current is passed through the wire. In principle this is quite simple. However, to meet the research objective, care had to be taken in the design of such a system.

The following were considered to be the requirements of the temperature measurement system:

1. Very small spatial resolution, on the order of the Kolmogorov microscale for temperature, $\leq$ 1 mm
2. Very high frequency response, DC to 2 khz
3. Very low velocity sensitivity, $\leq$ .0001 °C/(cm/sec)
4. Very low noise, equivalent temperature noise $\leq$ .005 °C rms
5. High temperature sensitivity, ~ 1 volt/°C.

Unfortunately several of these requirements impose conflicting constraints on the physical characteristics of the sensor and its associated electronics. The spatial resolution determines the

maximum sensor length while the required frequency response sets the maximum sensor diameter. Conflicts arise when trying to optimize the other requirements.

The sensor's maximum dimension will be its length, thus its length must be at least as small as the turbulent scale sizes at which thermal dissipation occurs. The temperature microscale is given by:

$$\eta_T = (D_T^3/\epsilon)^{1/4} \qquad (3-1)$$

Using typical values for D_T and ϵ we obtain,

$$\eta_T \approx 1 \text{ mm}$$

Using empirical relations the sensor frequency response can be obtained as a function of sensor diameter. The following relation (from Flow Corporation Publication No. 25) is used for a small cylindrical wire.

$$f(-3db) = \frac{(0.52+0.025\sqrt{\rho\bar{U}D}) \times 10^{-3}}{2\pi\rho c_p D^2} \qquad (3-2)$$

Taylor's hypothesis can be employed to determine the required frequency response based on the microscale. For typical velocities the value is about 1 khz. This corresponds to a maximum sensor diameter of about 1.5 μ. This diameter requirement dictates the use

of platinum as the wire material since it has a very high temperature coefficient of resistance and is available in these sizes. Only nickel has a higher temperature coefficient. However, it is not available in these small diameters.

Final selection of the sensor length and diameter and the current through the sensor was based on considerations of the noise level, velocity sensitivity and temperature sensitivity. The minimum noise level can be approximated by that induced by thermal effects. This relation is given by:

$$T_N = \frac{4}{I\alpha}\sqrt{\frac{kT\Delta F}{R}} \sim \frac{D}{IL} \qquad (3-3)$$

The bridge configuration determines the temperature sensitivity and is given by:

$$S = \frac{I\alpha R}{2} \sim \frac{IL}{D^2} \qquad (3-4)$$

The velocity sensitivity has been derived by Wyngaard (1971) and is given by:

$$C = \frac{I^2 R\ 0.25\,Re^{.45}}{\pi k L \bar{U}(.24+.56\,Re^{.45})^2} \sim \frac{I^2}{D^2} \qquad (3-5)$$

These relations result in a minimum value for L of .2 mm for the maximum allowable velocity sensitivity and noise level. In

addition it is found that the constraints are satisfied over a range of values of l/d and that the diameter should be as small as possible. Although Boston (1970) has reported use of sensors as small as 0.25 μ diameter it was felt that 0.5 μ diameter wire represented a reasonable compromise. For the 0.5 μ sensor, the length is 1 mm and the current level is 100 μa. These parameters resulted in a velocity sensitivity of 0.00006 °C/(cm/sec) and a noise level of 0.004° C rms.

The sensor construction was from Wollaston wire, which consists of a platinum wire of the desired diameter with a silver jacket. A short section of this wire was prestressed into a V-shape and soldered onto the sensor supports. The silver jacket was then electrochemically removed by placing the tip of the wire in a drop of dilute nitric acid at about 1.5 V DC potential. The silver jacket flakes off exposing the platinum case. Etching was continued until the desired sensor resistance was obtained. Figure 3-1 shows the details of this construction.

2. Velocity

Similar requirements are imposed on the velocity sensor system. These are all met with a commercially available constant temperature hot-wire anemometer (Thermo-Systems 1054A). With the hot-wire system the sensor diameter need not be as small as for

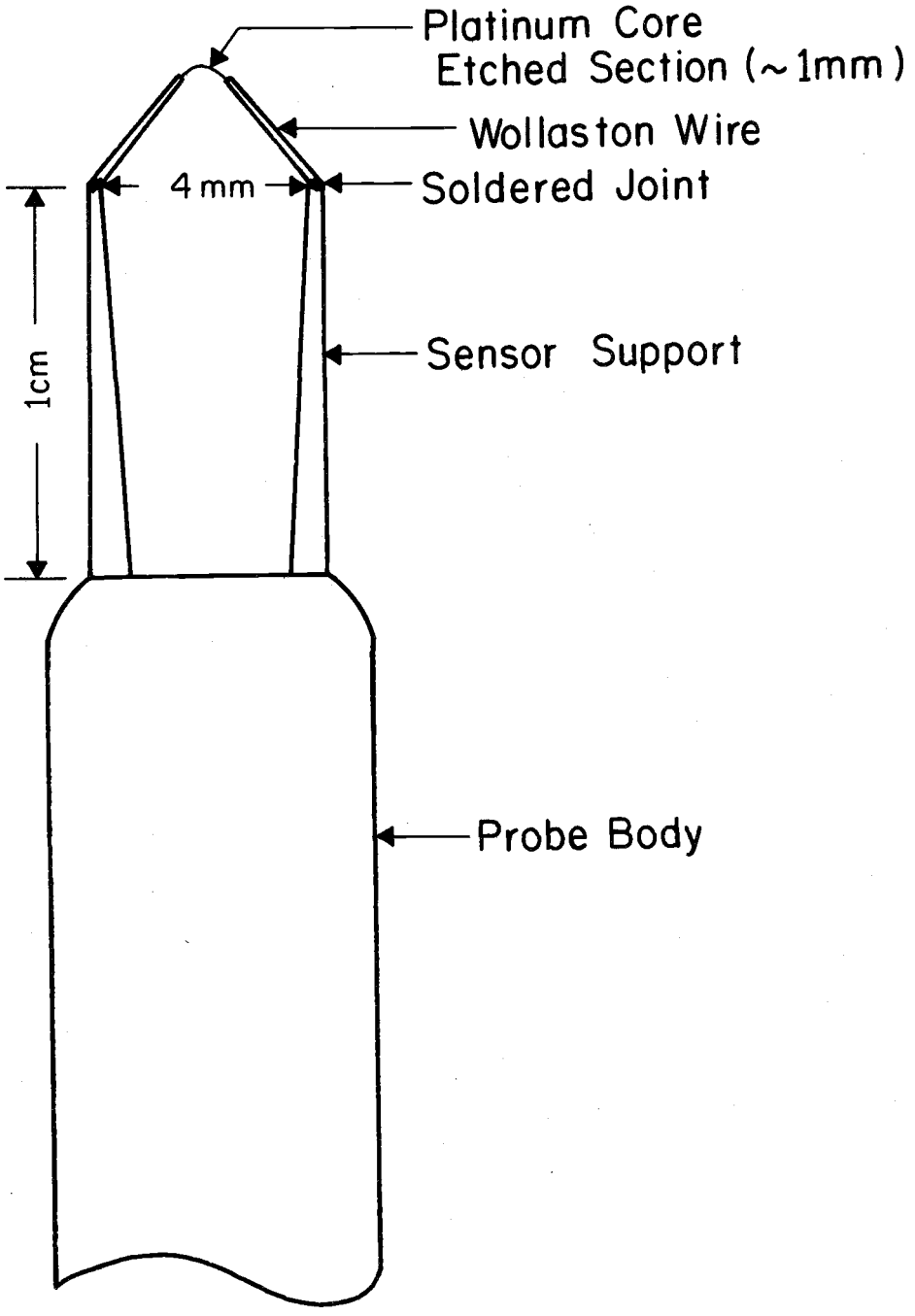

Figure 3-1. Construction Details of Platinum Resistance Thermometer.

temperature since the frequency response is not limited by the thermal inertia of the wire but is electronically limited. The system chosen had a sensor diameter of 1.37 μ and a length of .4 mm.

B. Temperature Sensor Electronics

The electronics package associated with the temperature sensor was developed over a period of two years to meet the requirements previously outlined. The requirement which resulted in the most difficulty was the noise level. Great care had to be taken in the design of the primary amplification stages to minimize the electronically induced noise levels.

1. Circuit Description

The platinum resistance thermometer (PRT) consists of three main sections: 1) the bridge and bridge voltage reference source, 2) the bridge amplifier, and 3) the detector, filter and output buffer stages. Figure 3-2 shows the simplified circuit schematic.

The bridge consists of four legs of approximately equal resistance, two reference resistors, the temperature probe and a balancing resistor. A capacitor in parallel with the balancing resistor allows the probe cable capacitance to be nulled. Relay circuitry (not shown) provides a means of switching calibration resistors in place of the probe and balancing legs of the bridge. This

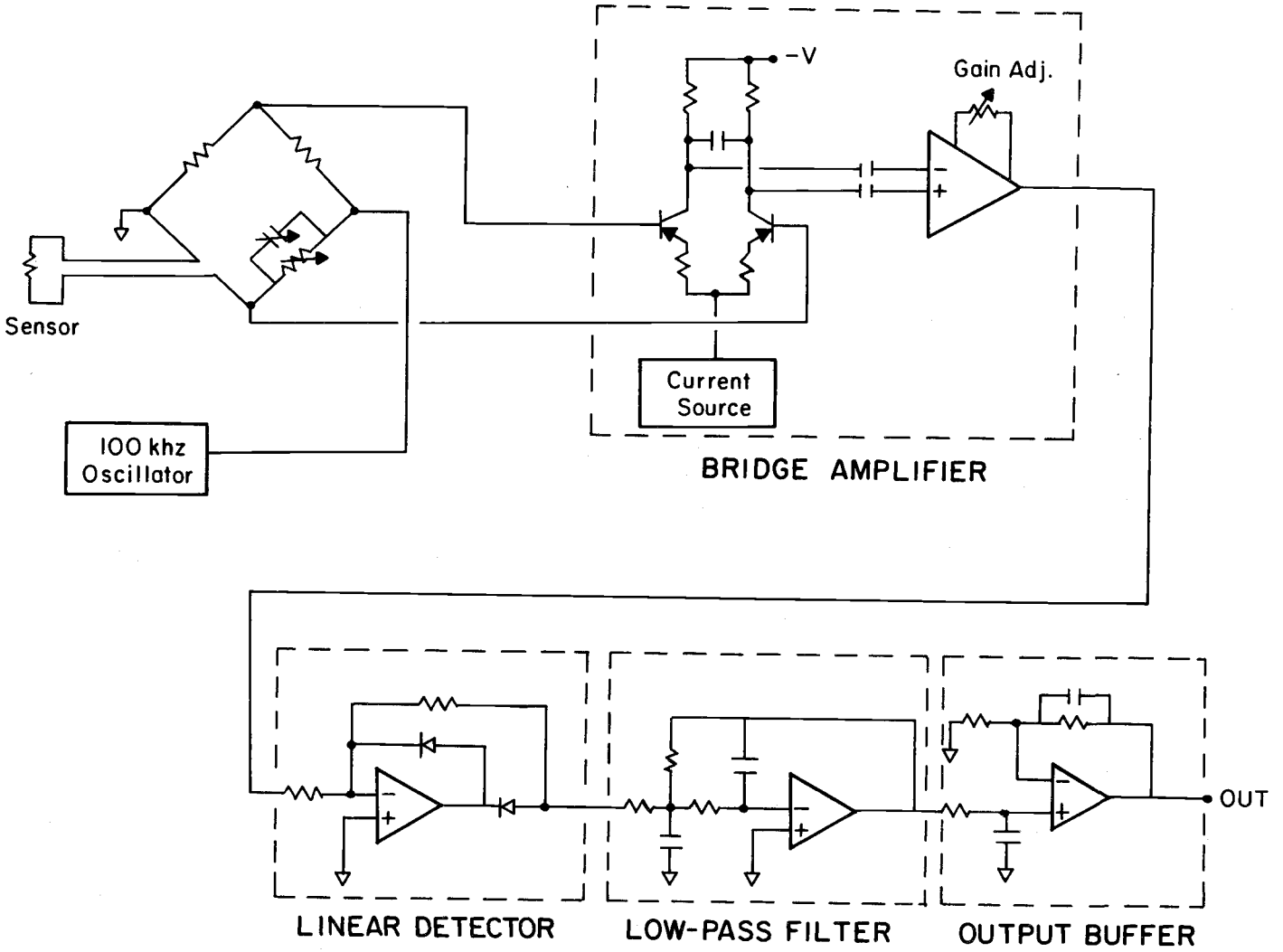

Figure 3-2. Simplified Schematic of Platinum Resistance Thermometer Electronics.

provides a check on the gain stability of the electronics.

The bridge is driven by a 100 khz sinusoidal signal. This signal is generated as a square wave with a pair of inverters through a regulated current source, which acts to regulate the amplitude stability. Frequency stability is provided by crystal control. The square wave is then fed through a 100 khz low pass filter where second and higher harmonics are attenuated. A low impedance driver then sends the signal to the bridge.

Any impedance imbalance in the bridge appears as an AC potential across the bridge. It is this potential which must be amplified and then rectified to produce a DC output proportional to the sensor temperature. The bridge signal is amplified by a low noise differential amplifier which consists of two stages, a discrete differential preamplifier followed by an integrated instrumentation amplifier. The superior low noise performance is determined by the first stage and great care was taken in the design of this stage. This pre-amplifier stage contains two principal features:

1. Optimum noise performance for a large range of source (sensor) resistance with a single resistor adjustment.
2. Unique temperature compensation to provide gain stability.

The pre-amplifier is a discrete differential amplifier using a low noise dual transistor driven by a constant current source. Noise performance of the transistor pair for a given source resistance is

dependent upon an optimum emitter current. The emitter current source design allows the current to increase proportionally with temperature. This is required to compensate the differential amplifier whose AC gain is inversely proportional to temperature. The compensated gain changes only 0.2% over a 0-70°C temperature range.

Additional gain is provided by an integrated instrumentation amplifier. This stage provides gain adjustment to obtain the desired output sensitivity.

The output of the instrumentation amplifier is a large amplitude, 100 khz sine wave. The amplitude of this signal is detected by the next stage which is a linear precision rectifier. The rectified output is then filtered with a 10 khz, two-pole, low pass filter to remove the 100 khz component. The filter output is buffered by a non-inverting output operational amplifier. Normal output is 0 to 10 volts DC.

Noise checks were made by using a temperature insensitive resistor in place of the sensor. The dummy probe's temperature was changed between room temperature (297°K) and that of liquid nitrogen (77°K). Measurements of the output noise at these temperatures then provided a measure of the noise figure of the PRT electronics. The noise figure is a figure of merit for noise performance of electronics. The maximum noise figure is 0 db while the best available amplifiers have optimum noise figures of about 1 db. The temperature tests resulted in a noise figure of 3.7 db. Total noise output of the PRT

electronics was 0.005 volts rms. This represents about 0.005°C rms.

2. Calibration

Calibration of the sensors and PRT electronics were performed by immersing the sensor in a temperature regulated bath of Freon-13. This procedure resulted in a calibration factor of 1.23 °C/volt with linearity to about 99% over a 12°C temperature range.

C. Differentiator Electronics

As previously noted the differentiator was employed to enhance the signal levels at the higher frequencies of interest. The primary consideration in this design was to minimize the noise level since any electronically generated noise in the bandpass of the filter would be amplified. Figure 3-3 shows a circuit schematic of the differentiator design. This consists of a unity gain input buffer. The next stage is a combined differentiator/integrator which produces a +20 db/decade transfer function (differentiation) for frequencies up to the "cutoff frequency." Above these frequencies there is a -20 db/decade frequency response (integration). The next stage is a three-pole, noninverting, low pass filter used to produce a sharper cutoff at frequencies above those of interest. The component values of the two filter stages were tailored to produce a linear transfer

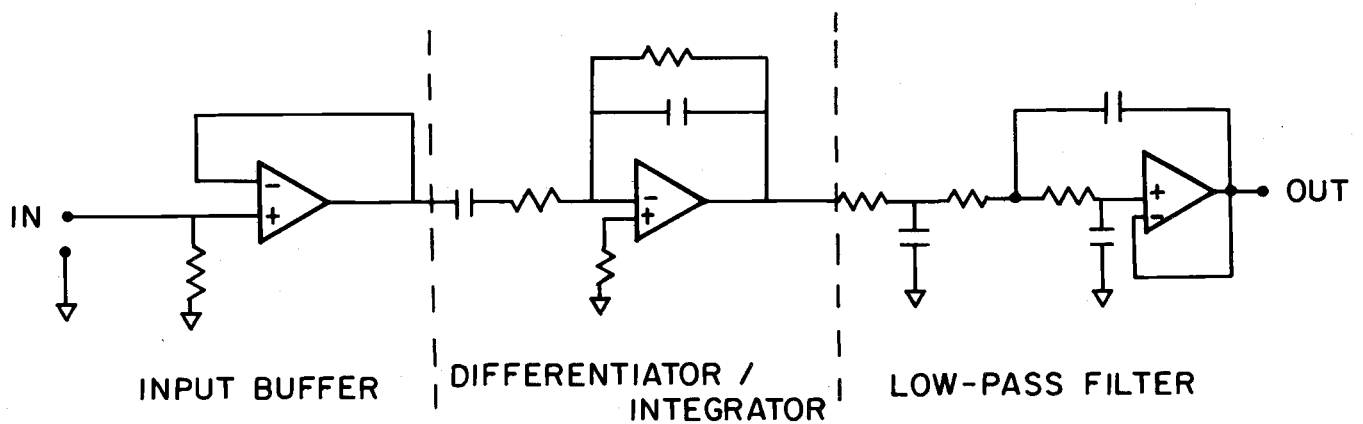

Figure 3-3. Simplified Schematic of Differentiator Electronics.

function with a slope of +20 db/decade up to the "cutoff" frequency, followed by a sharp cutoff. It was found that placement of the differentiating stage before the filter stage was critical for the achievement of the lowest noise design. Figure 3-4 shows the ideal and measured transfer functions for f_c = 2000 hz.

The hardware constructed allowed selection of one of six "cutoff" frequencies (100, 200, 400, 1000, 2000, or 4000 hz). The "cutoff" frequency used in the field experiment was 2000 hz.

D. Other Instrumentation

1. X-Wires

In addition to the single hot-wire a pair of crossed hot-film anemometers were used to determine the horizontal and vertical components of the wind velocity. These signals were used to directly measure the flux of momentum and with the temperature signal to determine the sensible heat flux. These sensors and associated electronics were also commercially available (Thermo-Systems Inc.).

2. Cup Anemometer

As an in situ calibration of the hot-wire anemometer a cup anemometer signal was simultaneously recorded. The system used was a low inertia Thornthwaite design. This had frequency response of about 1 hz.

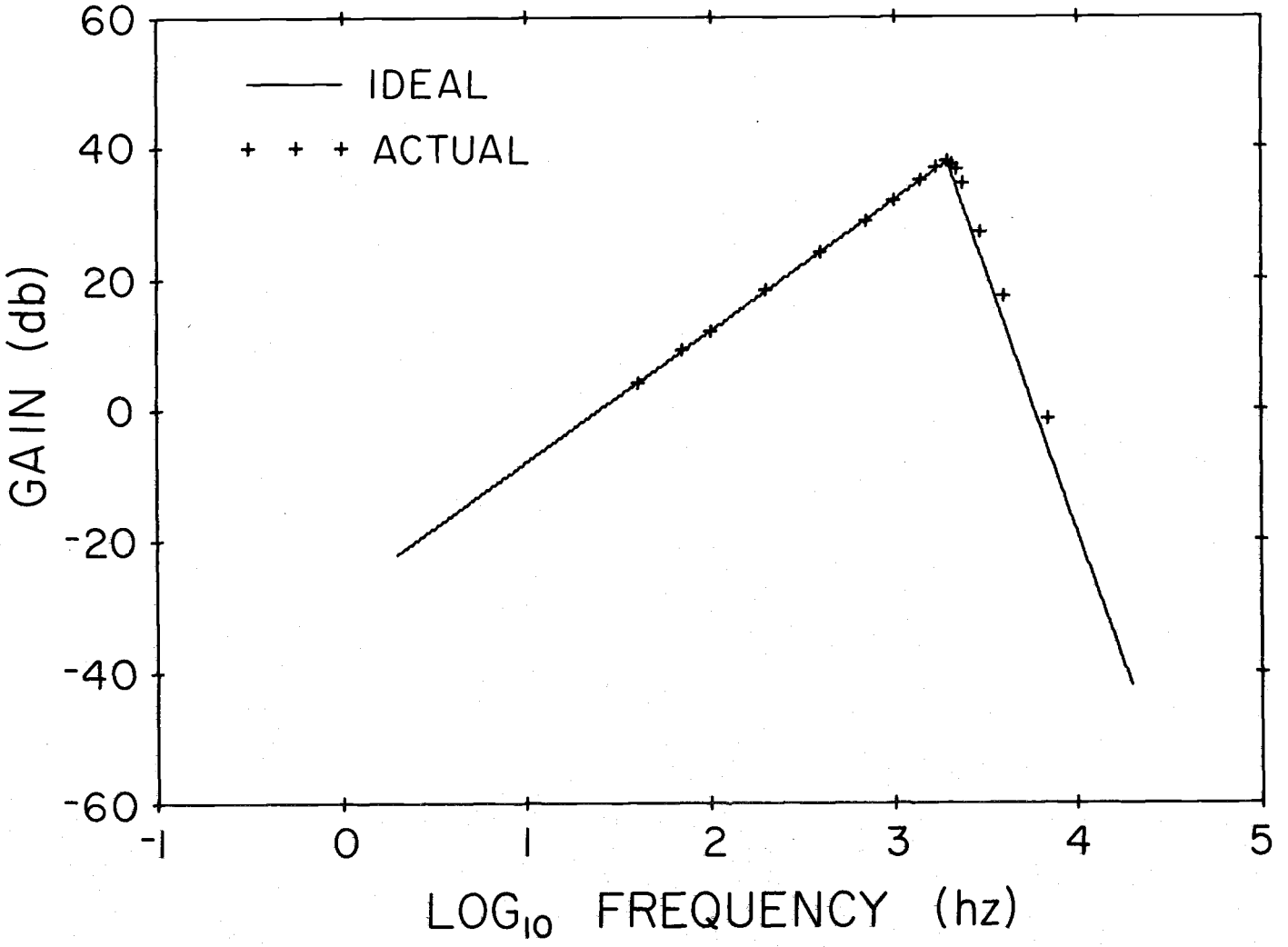

Figure 3-4. Ideal and Actual Differentiator Transfer Function.

3. Wind Vane

A fast response Thornthwaite wind vane was used to determine the wind direction so that the instrumentation could always be oriented into the direction of the mean wind.

E. Data Acquisition

1. Location

The site selected was over a very flat field of recently cut grass near Corvallis, Oregon. For the observed wind directions the fetch exceeded 1 mile. The primary reason for the selection of the site was the expectation of high sensible heat fluxes and hence of large temperature fluctuations. Measurements over the ocean present more stringent sensor requirements due to the much lower signal levels.

2. Mast Arrangement

All instruments were supported on a portable mast at a height of 2 meters. The mast could be rotated to maintain the sensor orientation into the mean wind. Figure 3-5 shows a picture of the mast arrangement. The signals from each sensor were carried by cable to an instrument hut approximately 100 feet downwind where they were conditioned and recorded.

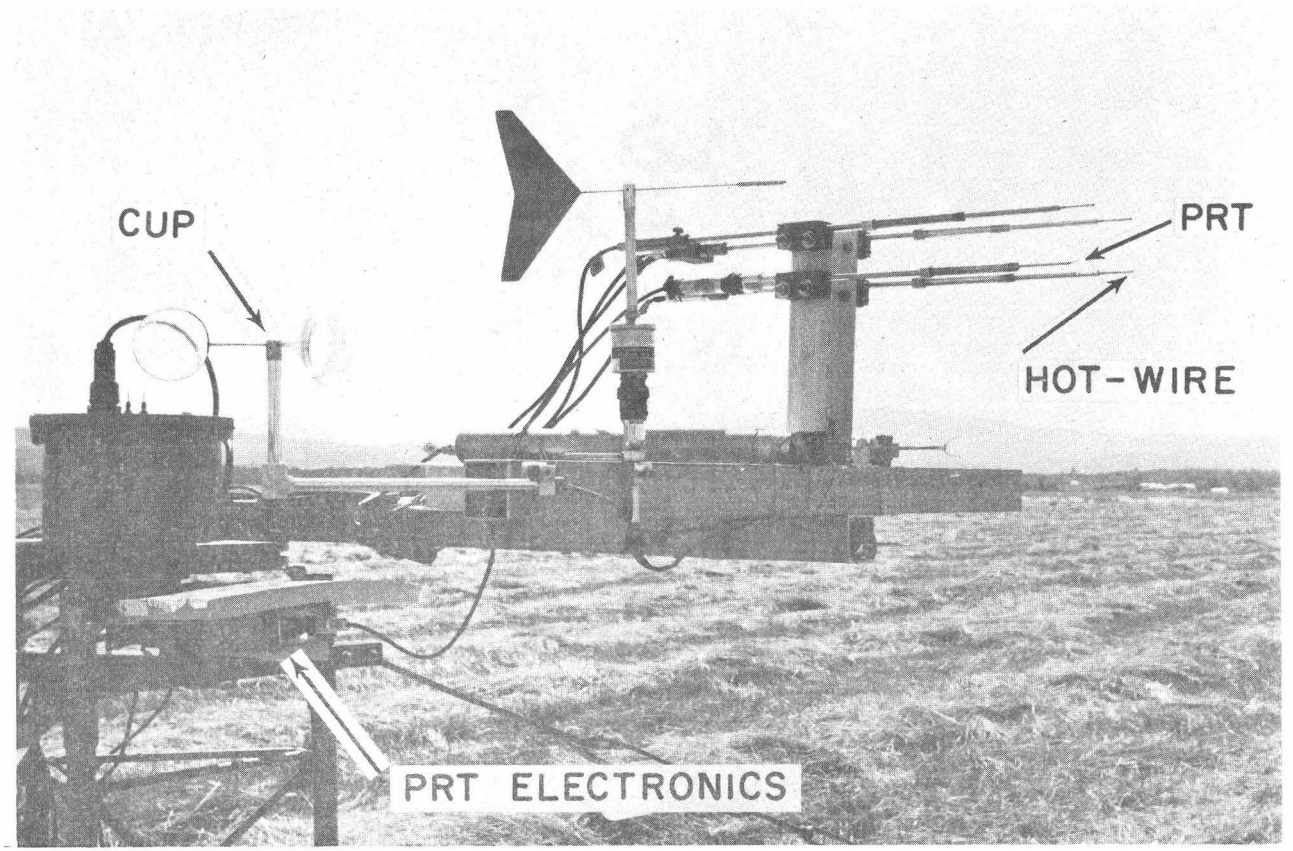

Figure 3-5. Instrument Mast.

3. Signal Conditioning and Recording

Prior to recording the signals in analog form on magnetic tape each was preconditioned to obtain the maximum dynamic range. Preconditioning essentially consisted of offsetting the mean voltage level and then amplifying or attenuating the fluctuating signals' levels to make them compatible with the tape recorder. The system is outlined in Figure 3-6.

The signals from the temperature sensor and hot-wire were recorded in two different ways. One tape recorder channel contained the undifferentiated signal output of the GAIN/OFFSET device. The other was differentiated prior to recording.

These signals together with the x-wire anemometer were recorded on separate FM (frequency modulated) channels of a magnetic tape recorder (Hewlett-Packard Model 3955). The cup anemometer and wind direction signals were passed through VCO's (voltage controlled oscillator), mixed and then recorded on a direct record channel. The recordings were made at 15 inches per second. At this speed the frequency response was flat to 5 khz and allowed a continuous 48 minute record to be made.

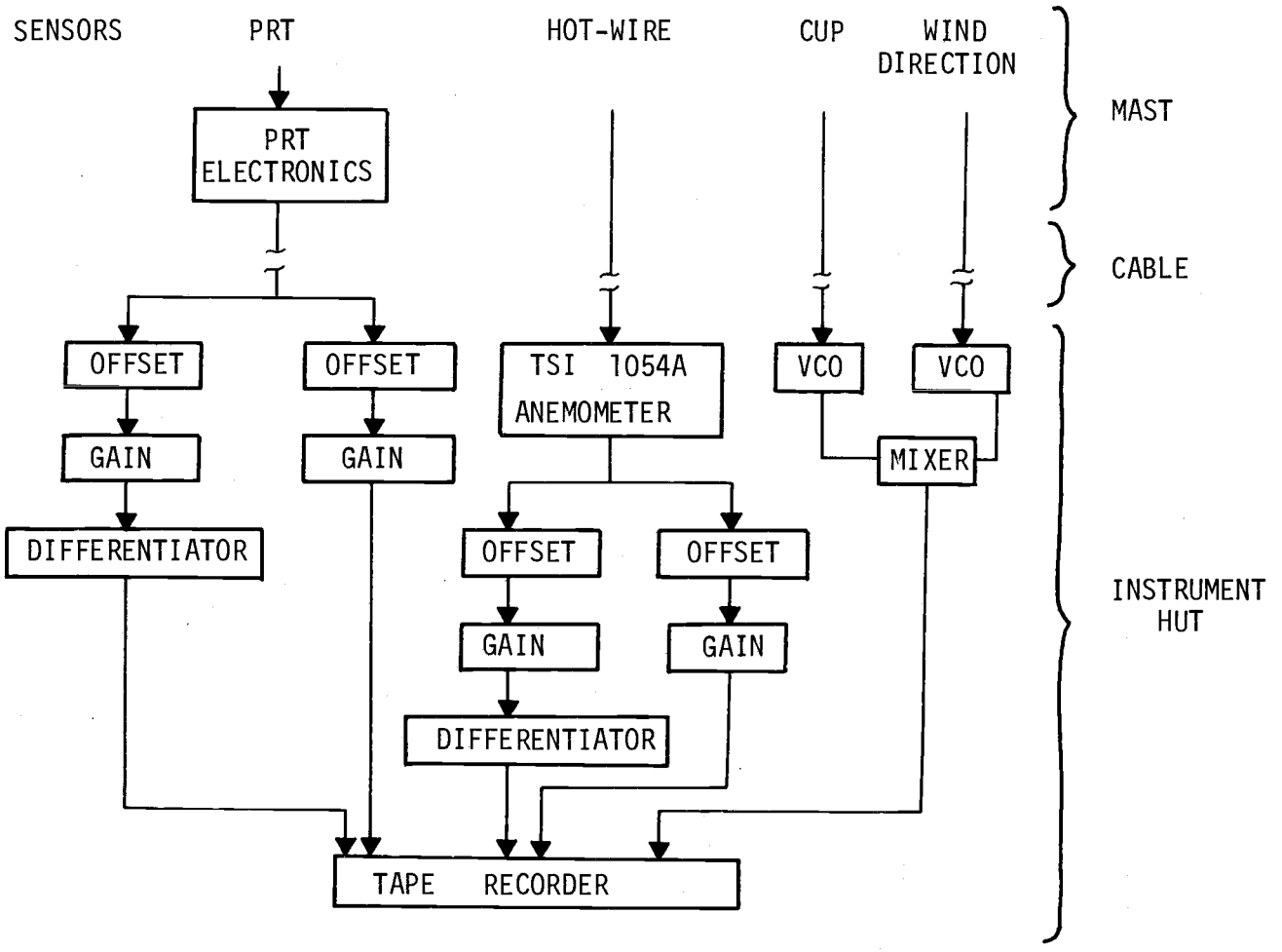

Figure 3-6. Block Diagram of Data Recording System.

IV. DATA ANALYSIS PROCEDURE

The data analysis consisted of three principal procedures. The first of these was to select sections of the recorded data which would be best for analysis. Next, these sections of analog information had to be converted into digital form. Finally the digital data had to be processed through various computer programs to obtain the desired results.

A. Data Selection

During the field experiment over 10 hours of data were recorded over a two day period. The data were recorded in sequence such that both stable and unstable conditions could be analyzed. To cover all of these stability conditions, sections of each tape were to be analyzed. Due to the intermittent nature of the temperature and velocity signals a time series of at least one minute is required to obtain a reasonable mean ratio of dissipation. Figure 4-1 shows the running-average rate of dissipation for averaging times up to 4 minutes. Strip chart recordings of the recorded signals were examined to find sections suitable for analysis. A typical strip chart recording is shown in Figure 4-2. Several criteria were used in the selection of these sections. Most important of these was that the signals of primary interest, the temperature and velocity derivatives, were

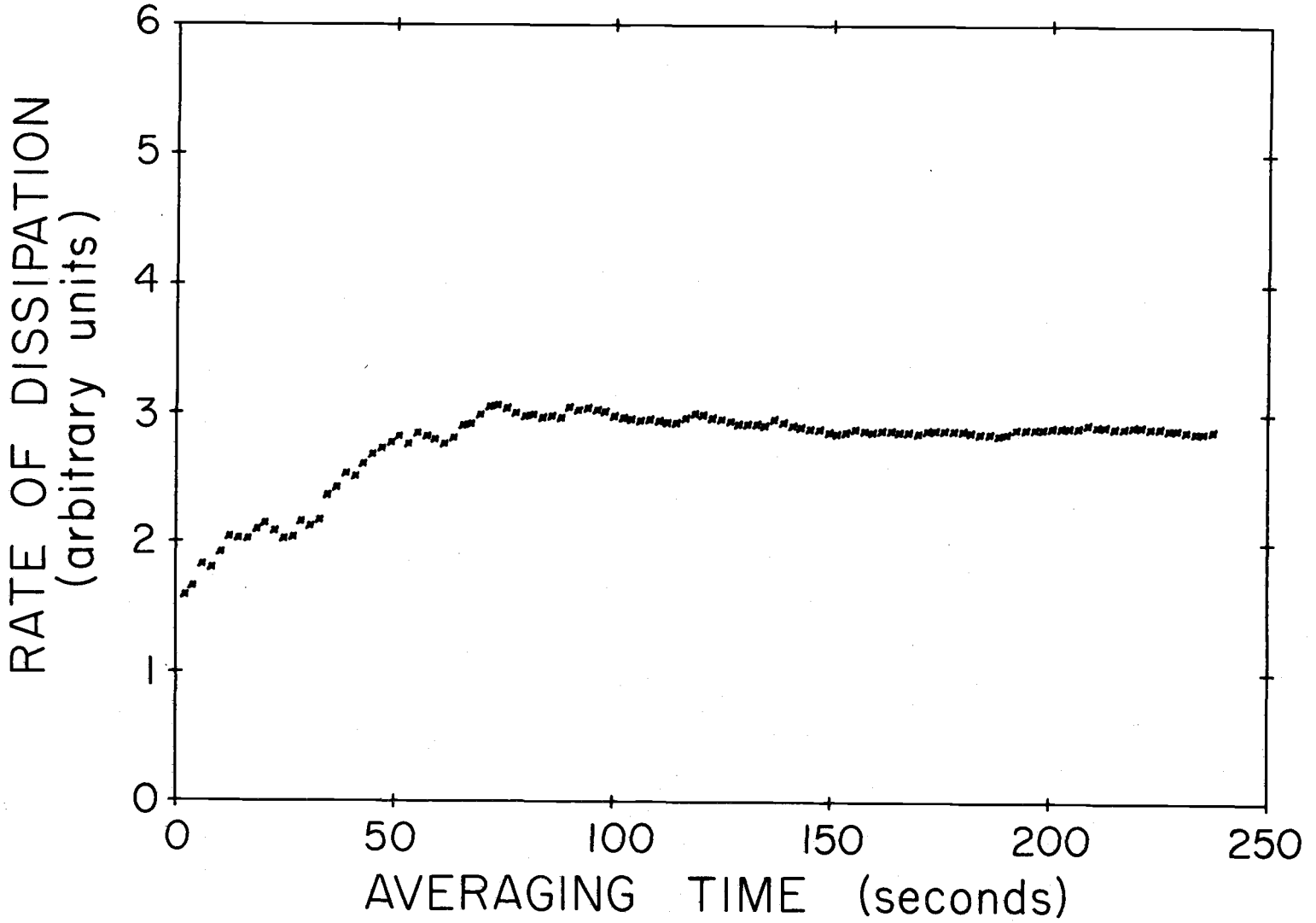

Figure 4-1. Effect of Averaging Time on Mean Rate of Temperature Dissipation.

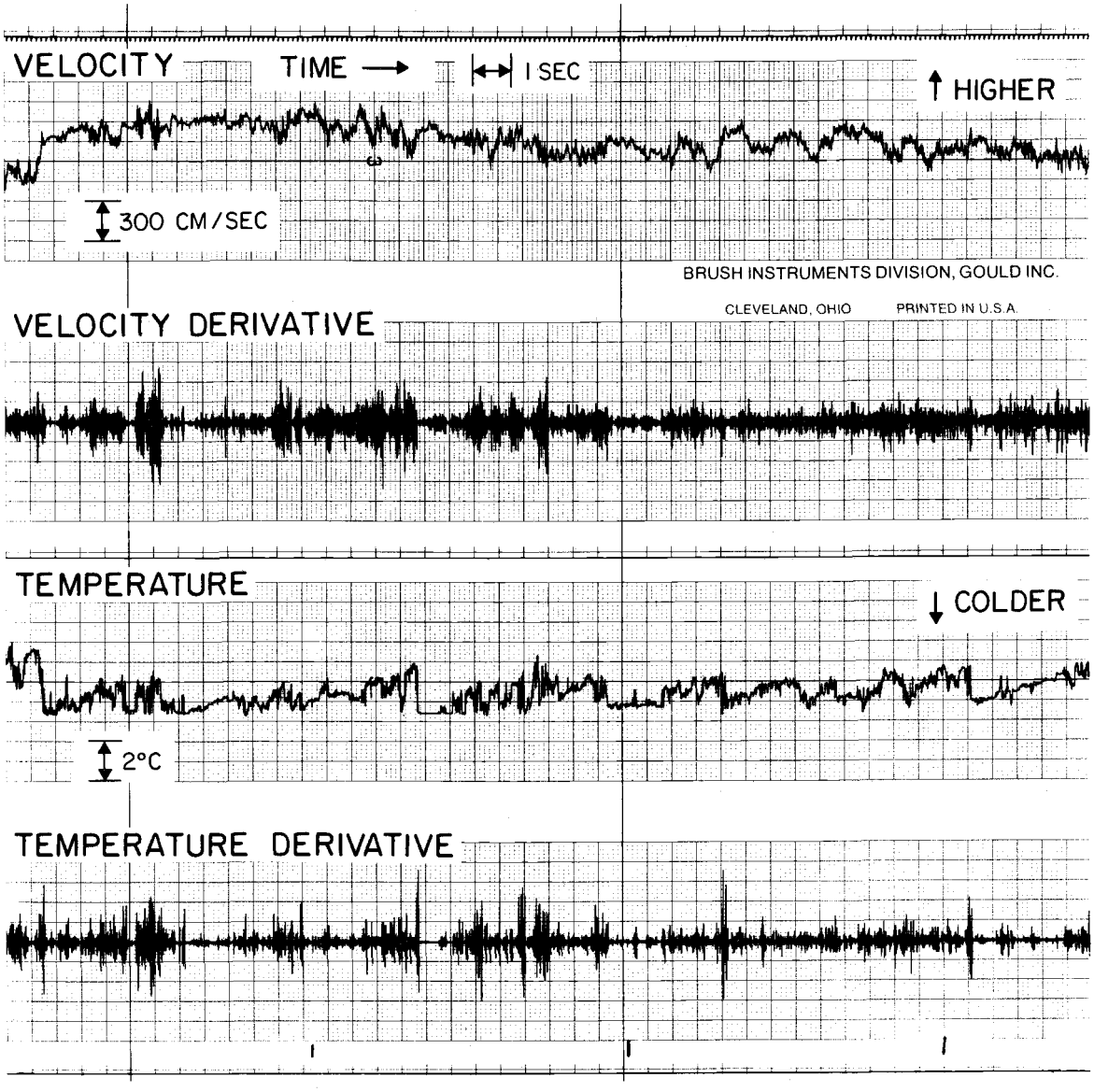

Figure 4-2. Typical Strip Chart Recording

without spurious spikes or other ambiguities. Selected sections also had to have nearly constant wind direction and wind velocity. A fiscal constraint limited the total time that could be analyzed to about 30 minutes; this represents about 30 million data words after digitizing.

Prior to final selection of sections for analysis all of the data was spectrally analyzed with an analog spectral analyzer (SAICOR-52B). This allowed much longer time series to be examined and gave preliminary spectral estimates for sections that were to be digitally analyzed.

The final data selection consisted of at least two one minute sections in each of the 14 data tapes. In addition to these, one 4 minute section was selected in each of six tapes.

Additional sections of longer length were selected from each tape for digitizing at lower frequencies. These signals were for the direct flux determination.

B. Analog-to-Digital Conversion

The selected analog data sections were converted to digital form using an EAI-640/680 hybrid computer. This machine had a dynamic range of ±10 v with digitized words of 12 bits including sign. To utilize this dynamic range the analog signals from the tape recorder were amplified before digitizing. Care was taken that this amplification would not produce any signals of greater than ±10 v. In addition

to amplifying, the signals were low pass filtered at one-half of the sampling frequency to prevent any aliasing.

For the high frequency data the signals were sampled at 4000 hz, which would allow spectral calculations to 2000 hz. The signals digitized at this frequency were the temperature, velocity, and their derivatives. The low frequency signals were digitized at 20 hz. These signals were the wind direction, cup anemometer velocity, hot-wire velocity, x-wire velocities, and PRT temperature.

C. Digital Analysis Programs

The entire high frequency analysis procedure is seen in Figure 4-3, showing the entire progression from raw analog data to final spectra and Kolmogorov constants. The analysis features for the low frequency data are similar and will not be discussed.

The first step in the analysis was to take the original analog-to-digital tapes and reformat them creating a new digital tape having data records of a length convenient for analysis. This length was chosen as 8192 words for the high frequency data. The Fast Fourier Transform (FFT) computer routine required the record size to be a power of 2 and 8192 is the largest such size which could be used on the available computer (CDC 3300). Since cross-spectra were to be computed on the low frequency data a record length of 4096 was chosen for that data.

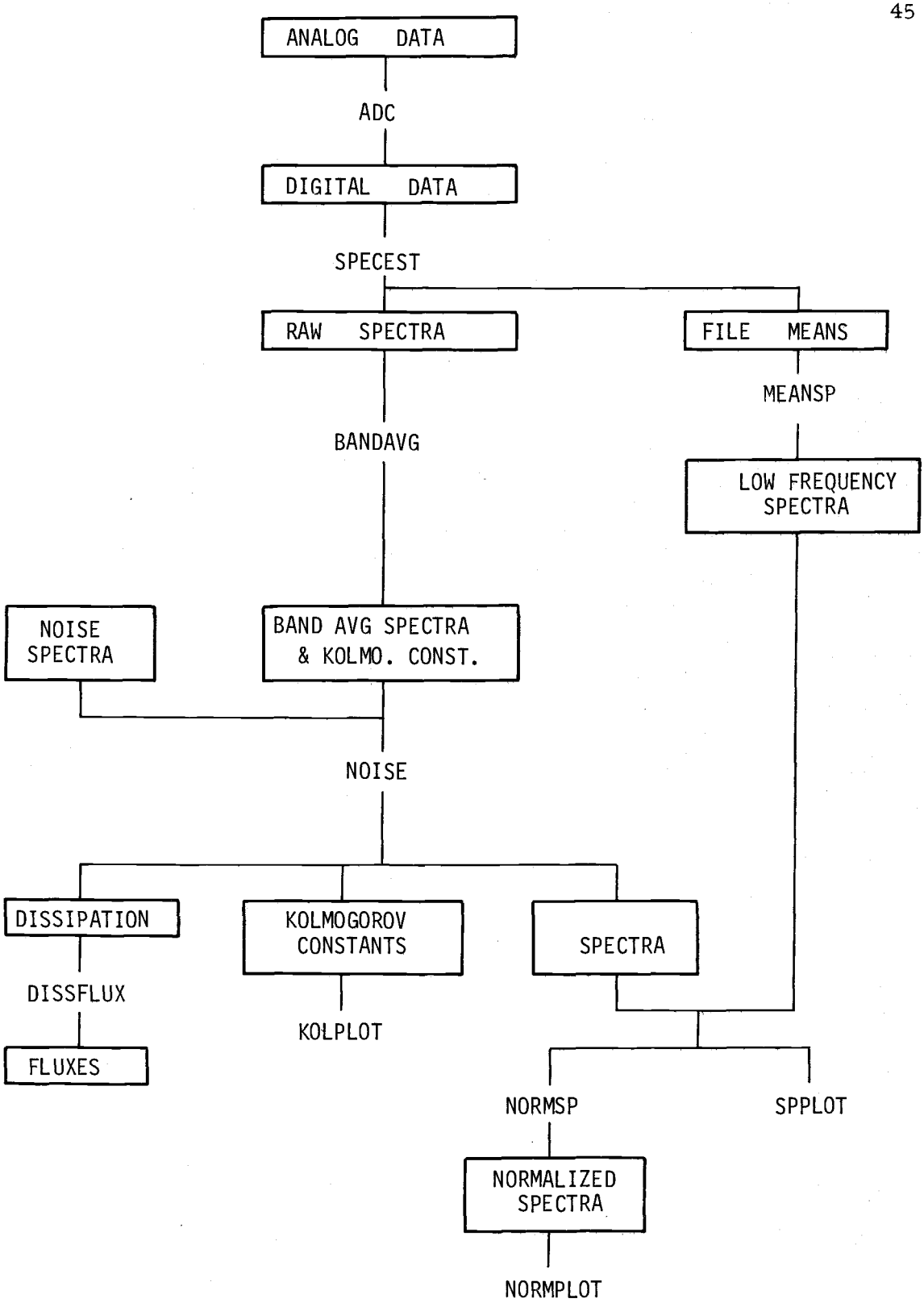

Figure 4-3. Block Diagram of Data Analysis Features.

The resulting reformated digital data tape generally consisted of about 115 files each having 4 records, one for each data channel, of 8192 integer words.

The next process was to use program SPECEST to calibrate the data, compute the Fourier coefficients for each record, and then compute the raw spectral estimates for each record. The basis of this program is the FFT routine to compute the Fourier coefficients. This is a library program which computes the Fourier coefficients using the Cooley-Tukey time decimation algorithm. This procedure requires significantly less time than a standard Fourier transform procedure.

Following calculation of the raw spectral estimates by SPECEST the data are ready for smoothing by the program BANDAVG. Due to the characteristic intermittency of the temperature and velocity fluctuations the raw spectral estimates of these signals are widely scattered. To improve the confidence in the spectral estimates, two techniques of smoothing are used. These are termed block and band averaging. The raw spectral estimates are first averaged over the total number of records making up a run. Further smoothing is accomplished by dividing the frequency range into equally spaced logarithmic frequency bands and averaging over all spectral estimates in each band. The band averaging scheme chosen consisted of 24 frequency bands with approximately 7 bands per decade of frequency.

Part of the program BANDAVG is used to determine the standard deviation and equivalent degrees of freedom for each spectral estimate. These can then be used to determine confidence limits on the spectral estimate. It can be seen (Jenkins and Watts, 1968) that $\nu S(f)/\Gamma(f)$ is a chi-square random variable with ν degrees of freedom.

Where:

$S(f)$ = averaged spectral estimate (4-1)

$\Gamma(f)$ = true spectral estimate

ν = equivalent degrees of freedom

$= 2(S(f))^2/\mathrm{Var}(S(f))$

Thus a $(1-\alpha)\cdot 100\%$ confidence interval is given by:

$$\frac{\nu S(f)}{\chi^2_U(\nu)} \leq \Gamma(f) \leq \frac{\nu S(f)}{\chi^2_L(\nu)} \qquad (4\text{-}2)$$

where: χ^2_U, χ^2_L are the upper and lower $\alpha/2$ points of the chi-square distribution.

Note that this interval is dependent on the value of the spectral estimates; however if we look at the confidence interval for the logarithm of the spectral estimate, we obtain a confidence interval length independent of the spectral estimate. This length of the confidence interval for log spectra is given by:

$$CI = \log_{10} (\chi_U^2(\nu)/\chi_L^2(\nu)) \qquad (4\text{-}3)$$

Figures 4-4 through 4-7 show typical spectra for the variable u, $\frac{\partial u}{\partial t}$, T and $\frac{\partial T}{\partial t}$ with 95% confidence intervals. These spectra differ from those presented in Chapter V in that they are not normalized. The low frequency spectral difference between the velocity and temperature spectra and their derivative spectra is attributed to low frequency noise generated in the differentiators, which is inversely proportional to the frequency.

The program BANDAVG also calculates raw estimates of the Kolmogorov constants and then band averages these estimates. This procedure is used to take advantage of the expected prewhitened condition of the Kolmogorov constants in the frequency range of interest.

Following BANDAVG spectral corrections are made for the noise contribution to the spectrum by program NOISE.

Noise corrections are accomplished by taking advantage of the intermittency characteristic. The spectra of records taken during quiet periods should be representative of the noise spectra level. This level is then subtracted from the measured spectra to obtain a true spectrum.

Several intermittent sections from each tape were analyzed to determine the noise levels. It was found that in general this correction was very small ($< 1\%$), only in the temperature measurements

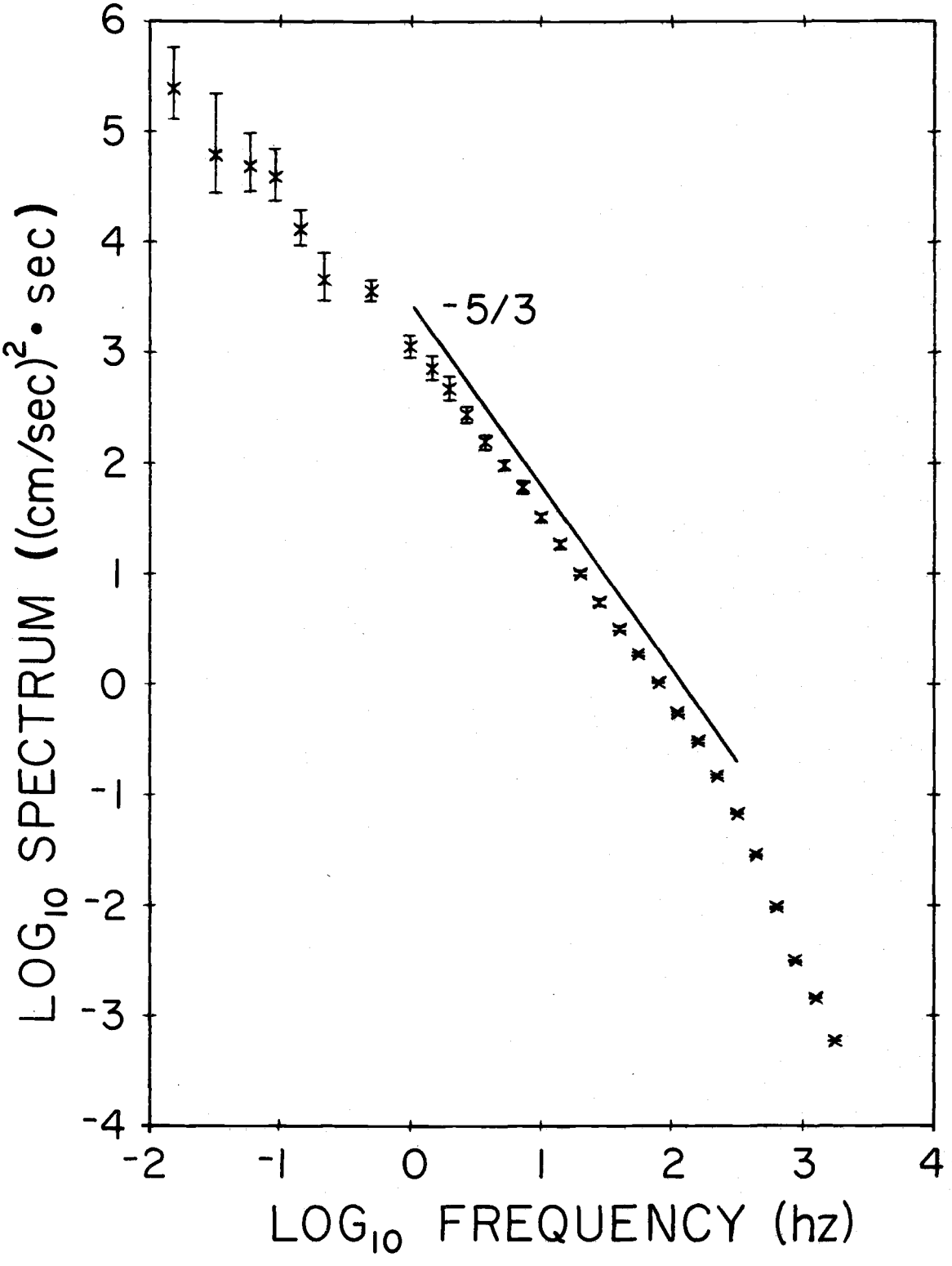

Figure 4-4. Typical Spectrum of Horizontal Wind Velocity (with 95% confidence intervals).

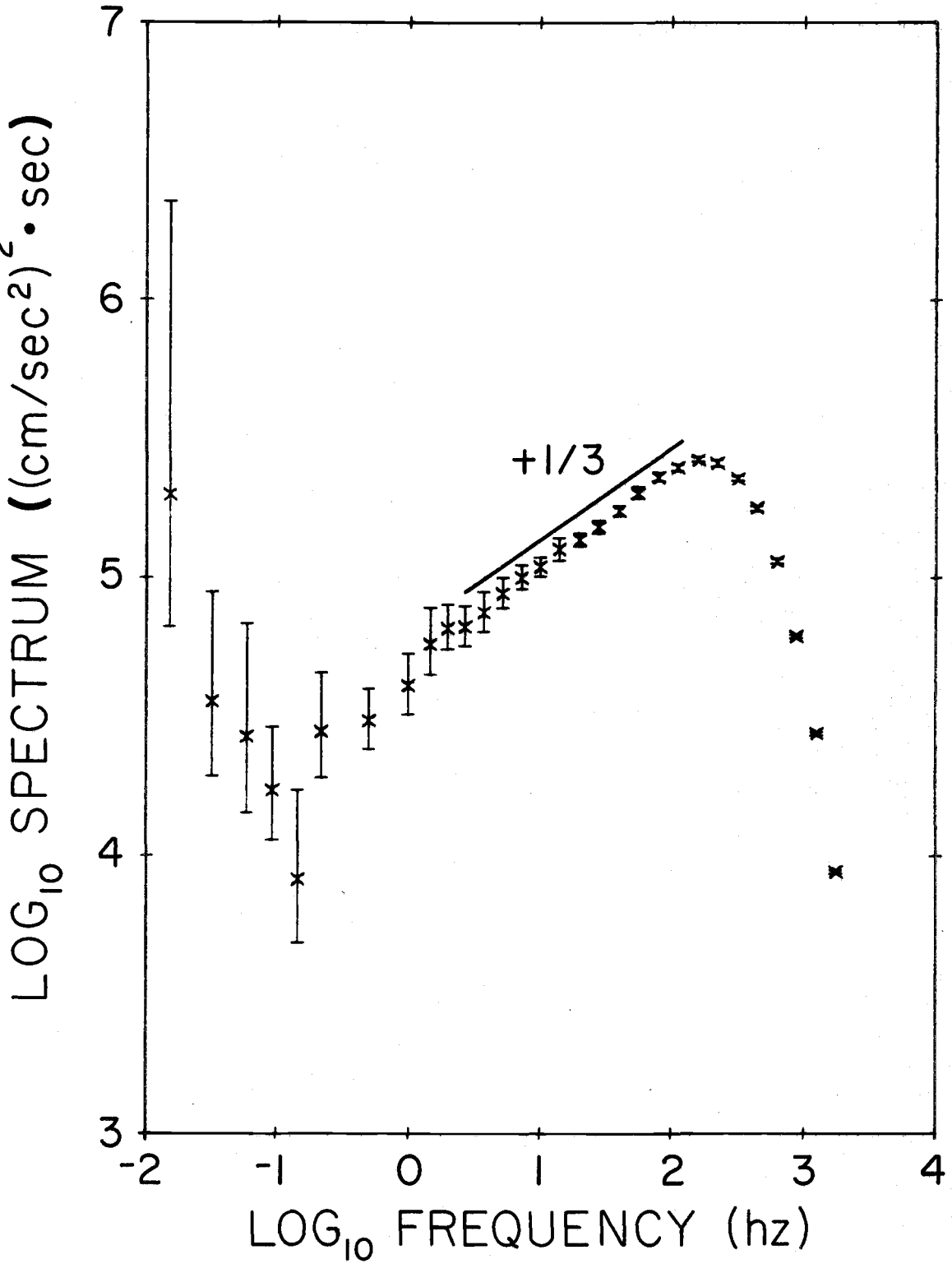

Figure 4-5. Typical Spectrum of Wind Velocity Derivative (with 95% confidence intervals).

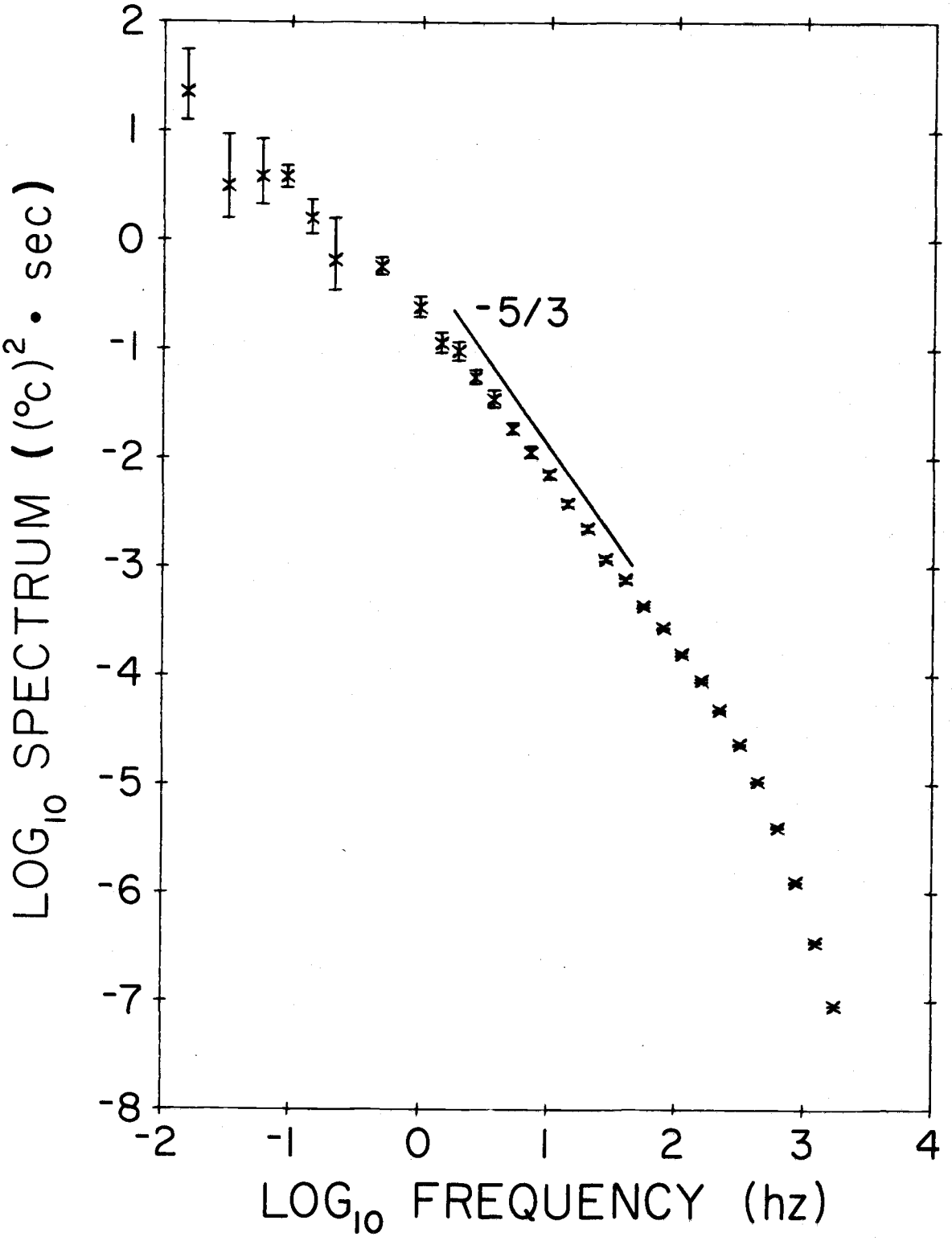

Figure 4-6. Typical Spectrum of Air Temperature (with 95% confidence intervals).

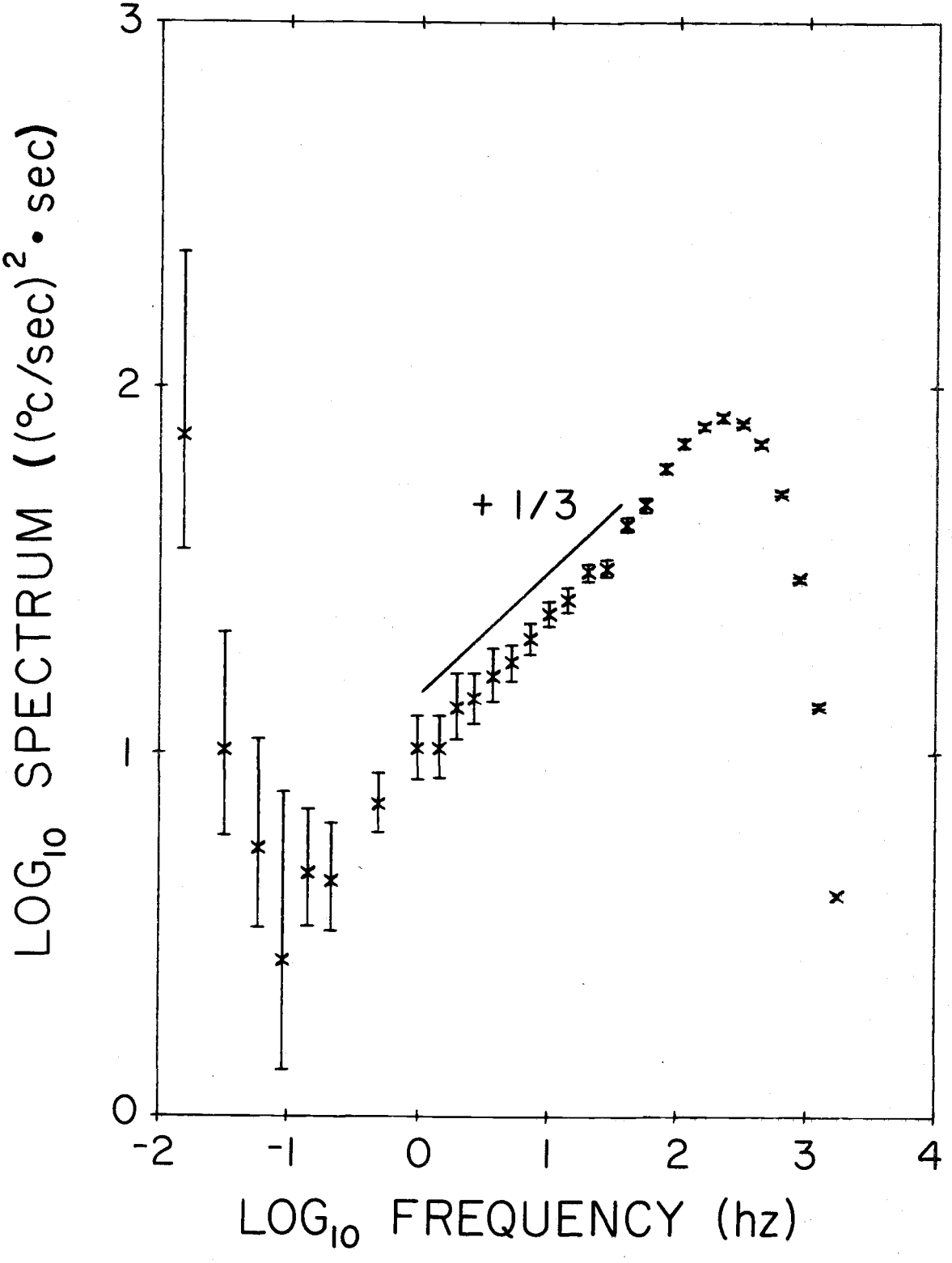

Figure 4-7. Typical Spectrum of Air Temperature Derivative (with 95% confidence intervals).

under nearly neutral conditions did the noise level represent an appreciable contribution to the measured spectrum. Figure 4-8 shows a measured spectrum and the corrected spectrum for the temperature derivative signal. The rather prominent noise peak at about 6 hz was found on all runs but as can be seen it is of the proper magnitude to correct the measured spectrum. An explanation of noise energy at this frequency has not been found but it must be associated with the differentiator electronics since only the derivative signals have this noise peak.

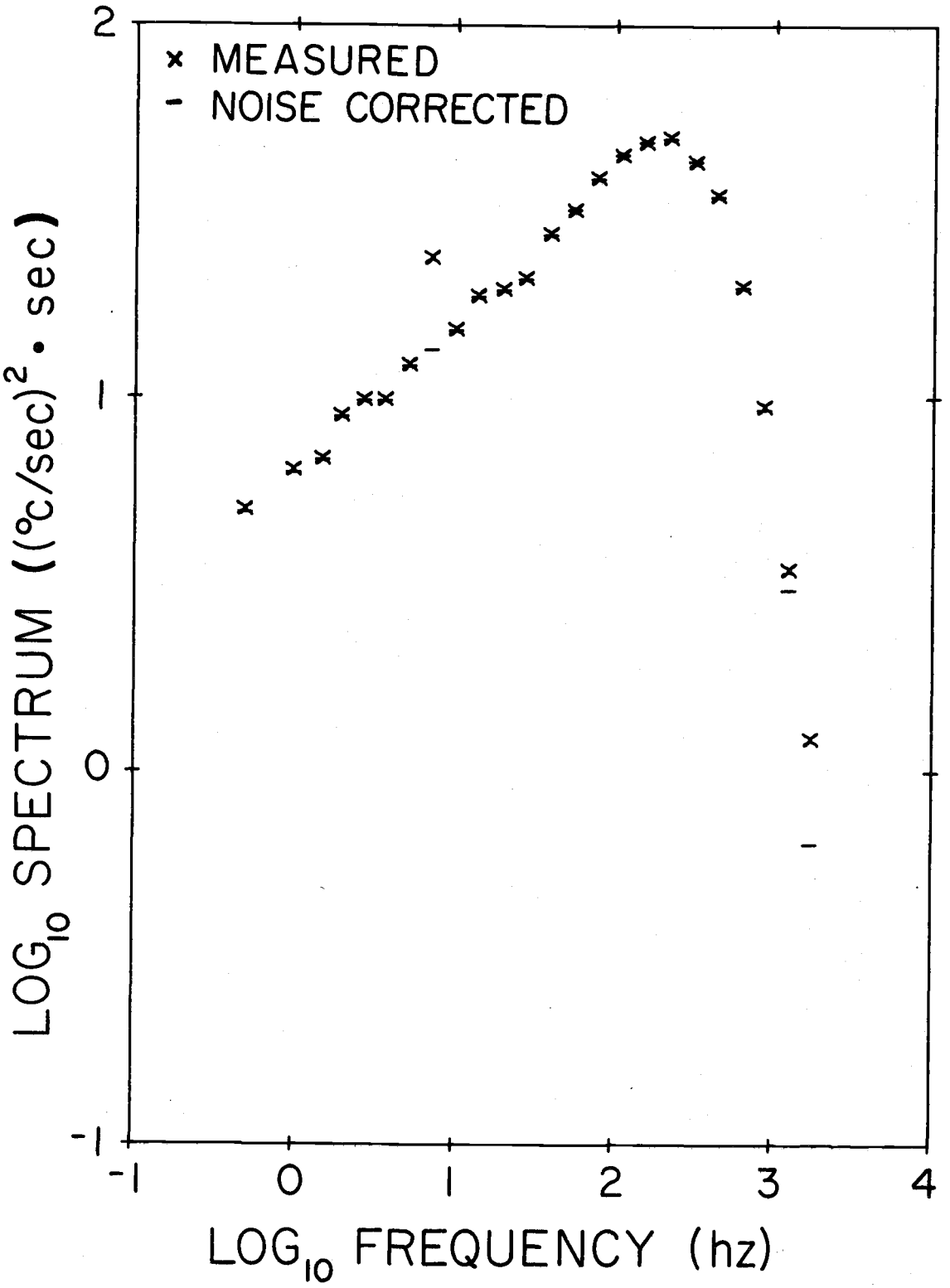

Figure 4-8. Effect of Noise Correlation on Typical Temperature Derivative Spectrum.

V. RESULTS

Data sections were analyzed from nine different runs. Table 5-1 summarizes these runs and the conditions present for each. As can be seen the Reynolds' number is typically about $.5 \times 10^6$ and the stability parameter, z/L, varies from -.1 to +.035. The record length was taken as about 4 minutes for about one-half of the runs. These runs were those with the best signal to noise ratios. Other runs were analyzed with about 1.5 minute record lengths.

Table 5-1. Summary of run conditions (July, 1973; z = 200 cm).

Run No.	$\bar{U}$ (cm/sec)	Re x 10^{-6}	z/L	Record Length (sec)
RY21C	329	.406	+.035	237.6
RY22A	452	.558	-.100	233.5
RY23B	490	.605	-.078	237.6
RY24B	537	.663	-.059	235.5
RY25C	590	.728	-.044	237.6
RY26B	602	.743	-.037	237.6
RY27A	592	.731	-.027	75.8
B	575	.710	-.025	77.8
RY28A	391	.483	-.045	77.8
B	345	.426	-.018	77.8
RY29A	344	.425	-.006	77.8
B	324	.400	-.006	77.8
C	297	.367	+.023	77.8

Subsequent sections will discuss the velocity spectra, the temperature spectra and the flux comparison.

A. The Velocity Spectrum

The velocity and velocity derivative spectra were used to determine the mean rate of dissipation of turbulent kinetic energy, ϵ, and the Kolmogorov constant for velocity, α. Integration of the velocity derivative spectrum yields the dissipation, Eqn. (1-26). The constant, α, was then calculated using Eqn. (1-34). Table 5-2 summarizes the results for each run. Based on 13 estimates a value of 0.504, with a standard error of the mean equal 0.007, was obtained. This value agrees well with most of the previous estimates. Figure 5-1 shows the average of α over all runs as a function of frequency with 95% confidence intervals. The band-averaged value of α in Table 5-2 was obtained by averaging all estimates between about 1hz and 28 hz.

Velocity spectra were normalized according to Eqn. (1-18). This permits comparison of the spectra from all runs. Existence of a universal spectral function would result in a single curve for all data points. Figure 5-2 is a composite normalized plot of all data. As can be seen a universal function does appear to exist, but this has been verified before, so what is indicated is that the data were recorded and analyzed properly.

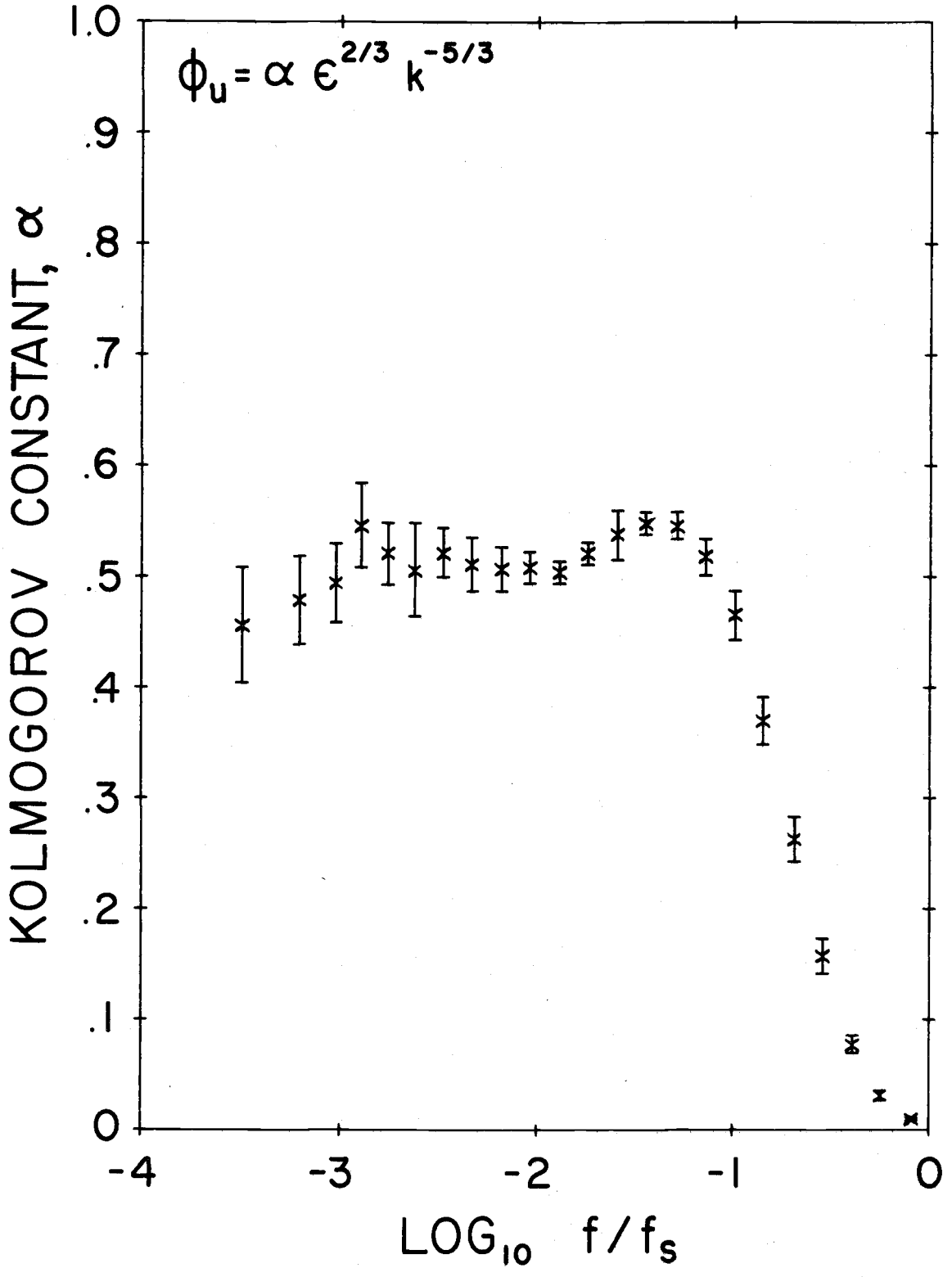

Figure 5-1. Frequency Variation of One-Dimensional Kolmogorov Constant for Velocity (with 95% confidence intervals).

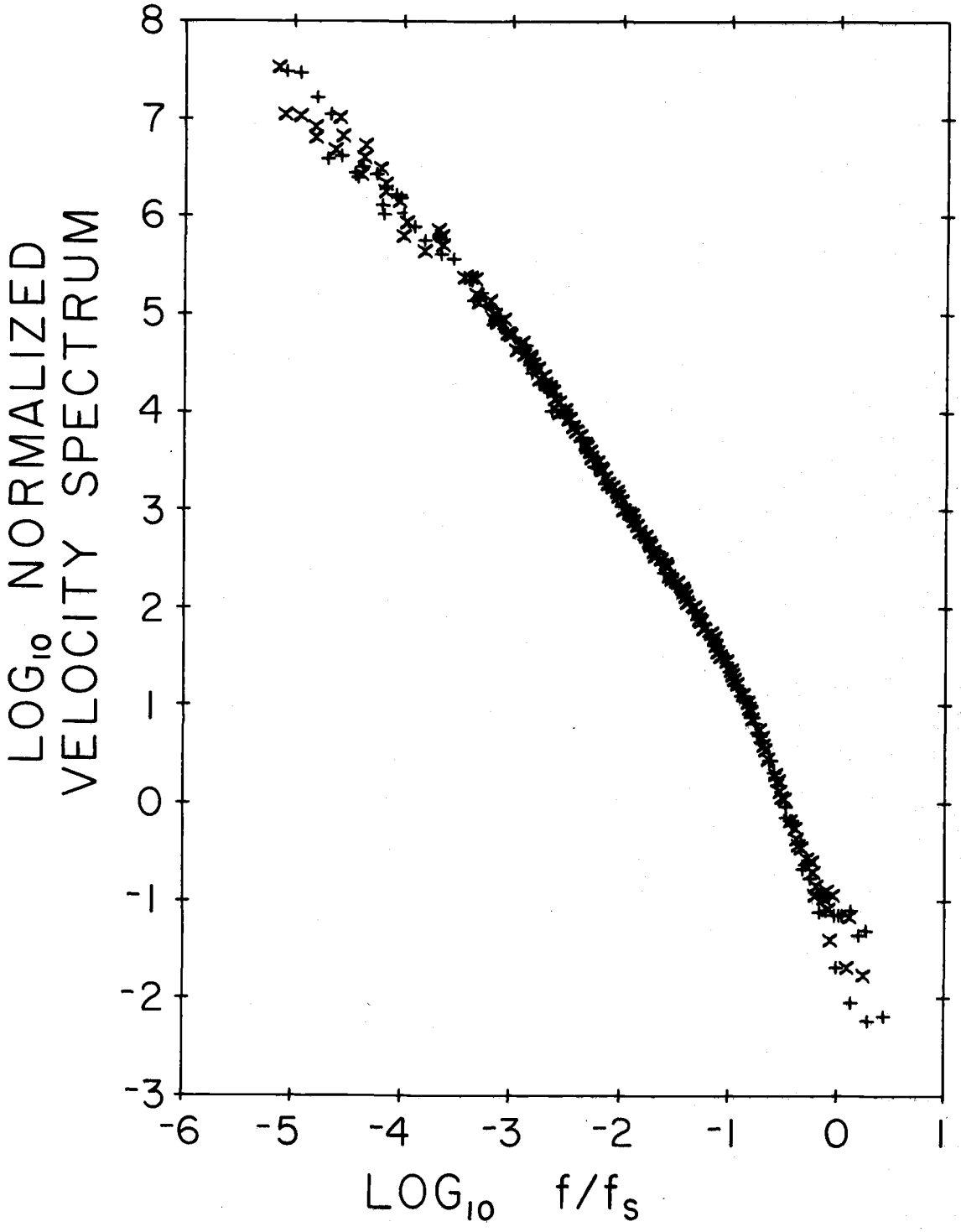

Figure 5-2. Composite Normalized Velocity Spectra.

Table 5-2. The one-dimensional Kolmogorov constant for velocity.

Run No.	z/L	ϵ (cm^2/sec^3)	α (10 hz)	α (1-28 hz)
RY21C	+.035	392	.514	.525
RY22A	-.100	609	.496	.500
RY23B	-.078	994	.512	.516
RY24B	-.059	1379	.516	.505
RY25C	-.044	1535	.520	.511
RY26B	-.037	1628	.518	.518
RY27A	-.027	1656	.497	.486
B	-.025	1419	.520	.543
RY28A	-.045	471	.489	.522
B	-.018	544	.518	.529
RY29A	-.006	396	.450	.493
B	-.006	324	.488	.454
C	+.023	157	.516	.532
		Average	.504	.510
		Standard deviation	.026	.063
		Standard error of mean	.007	.005

The velocity derivative spectra were normalized according to Eqns. (1-16) and (1-18). As was previously noted the spectra of the velocity derivative is directly related to k^2 times the spectra of the velocity (i.e. to the velocity dissipation spectra). Figure 5-3 is a plot of the normalized velocity dissipation spectra. Again the existence of a universal function is verified.

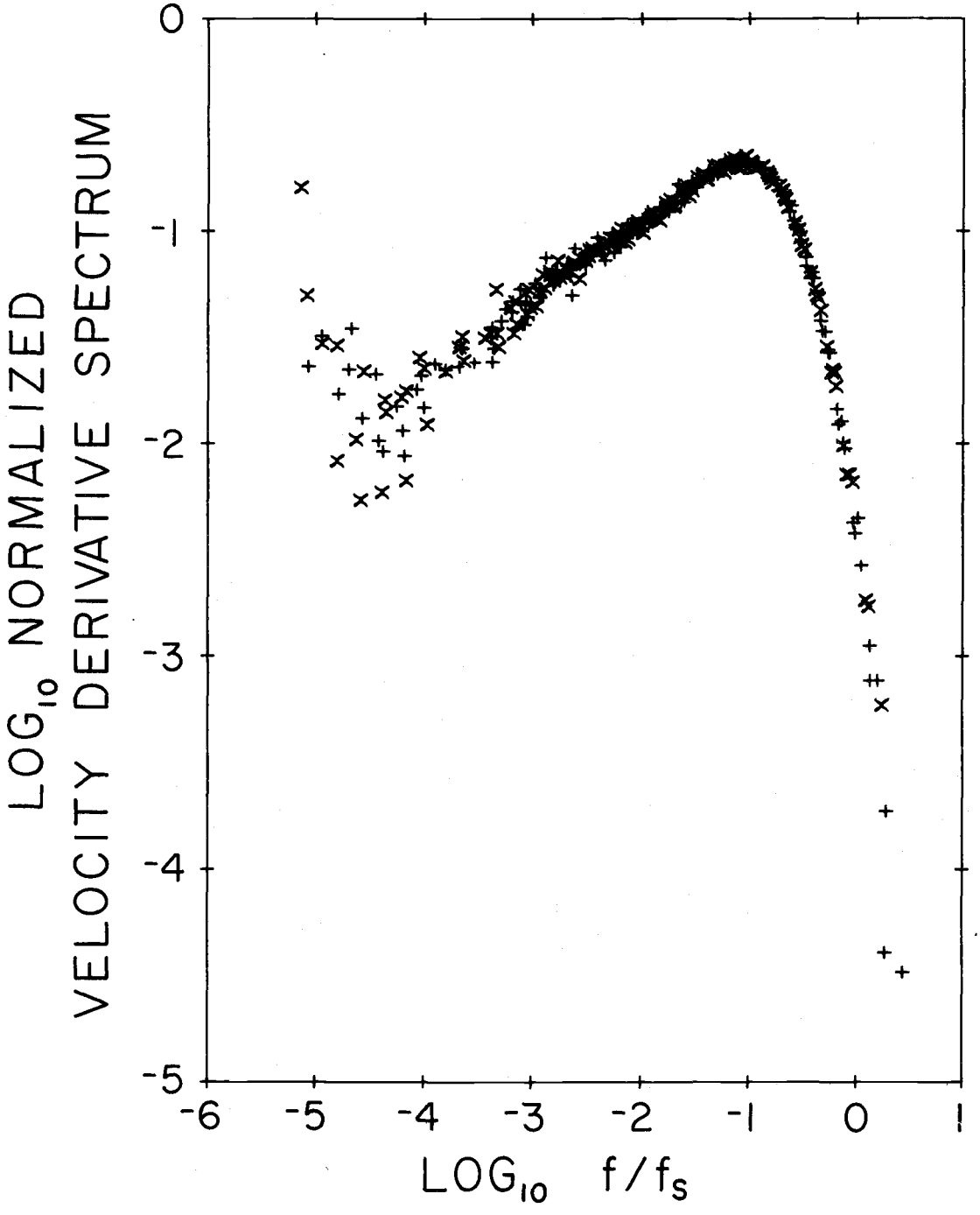

Figure 5-3. Composite Normalized Velocity Derivative Spectra (Energy Dissipation Spectra).

B. The Temperature Spectrum

The temperature spectrum results were used to determine the mean rate of dissipation of temperature variance. This was used with the previously calculated kinetic energy dissipation to calculate the Kolmogorov constant for temperature, β. Integration of the temperature derivative signal was used to determine the dissipation, Eqn.(1-31). The constant, β, was then calculated using Eqn. (1-36). Table 5-3 summarizes the results for each run. No values were estimated for RUNS RY29A & B due to the very low signal levels during these runs. Based on 11 estimates a value of 1.02 was obtained, with a standard error of the mean equal .03. This value is nearer to the value 0.8 reported by several researchers than the recent values of Boston (1970) and Gibson, et al.(1970) which were 1.6 and 2.3 respectively. Both Boston and Gibson, et al. used the direct approach used here. Figure 5-4 shows the average of β over all runs with 95% confidence intervals. The band averaged value of β in Table 5-2 was obtained by averaging all estimates between about 5 hz and 28 hz.

Temperature spectra were normalized according to Eqn. (1-20). Since only one fluid was used no normalization with respect to the Prandtl number is required. Figure 5-5 is a composite normalized plot of the spectra. The existence of a universal function for

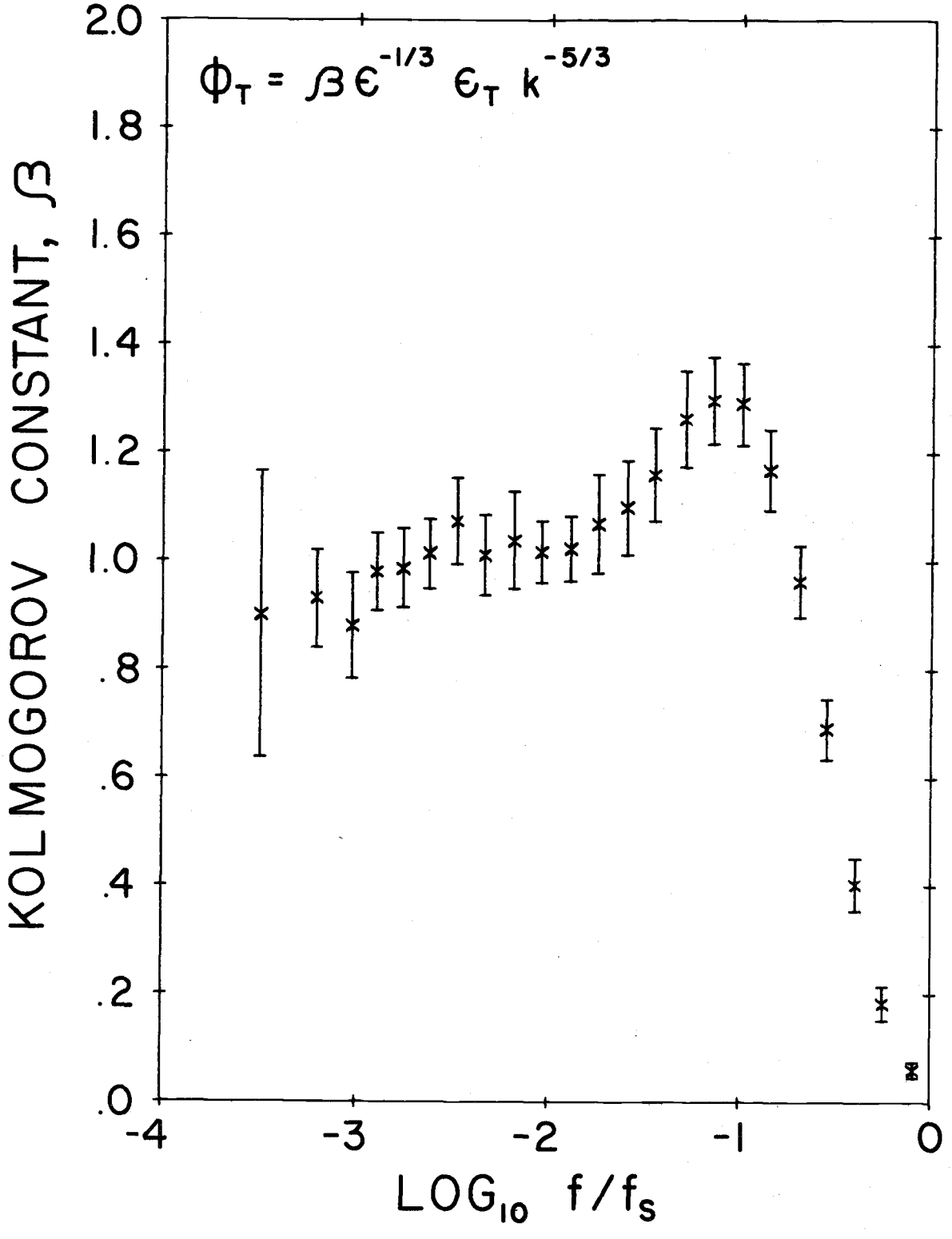

Figure 5-4. Frequency Variation of One-Dimensional Kolmogorov Constant for Temperature (with 95% confidence intervals).

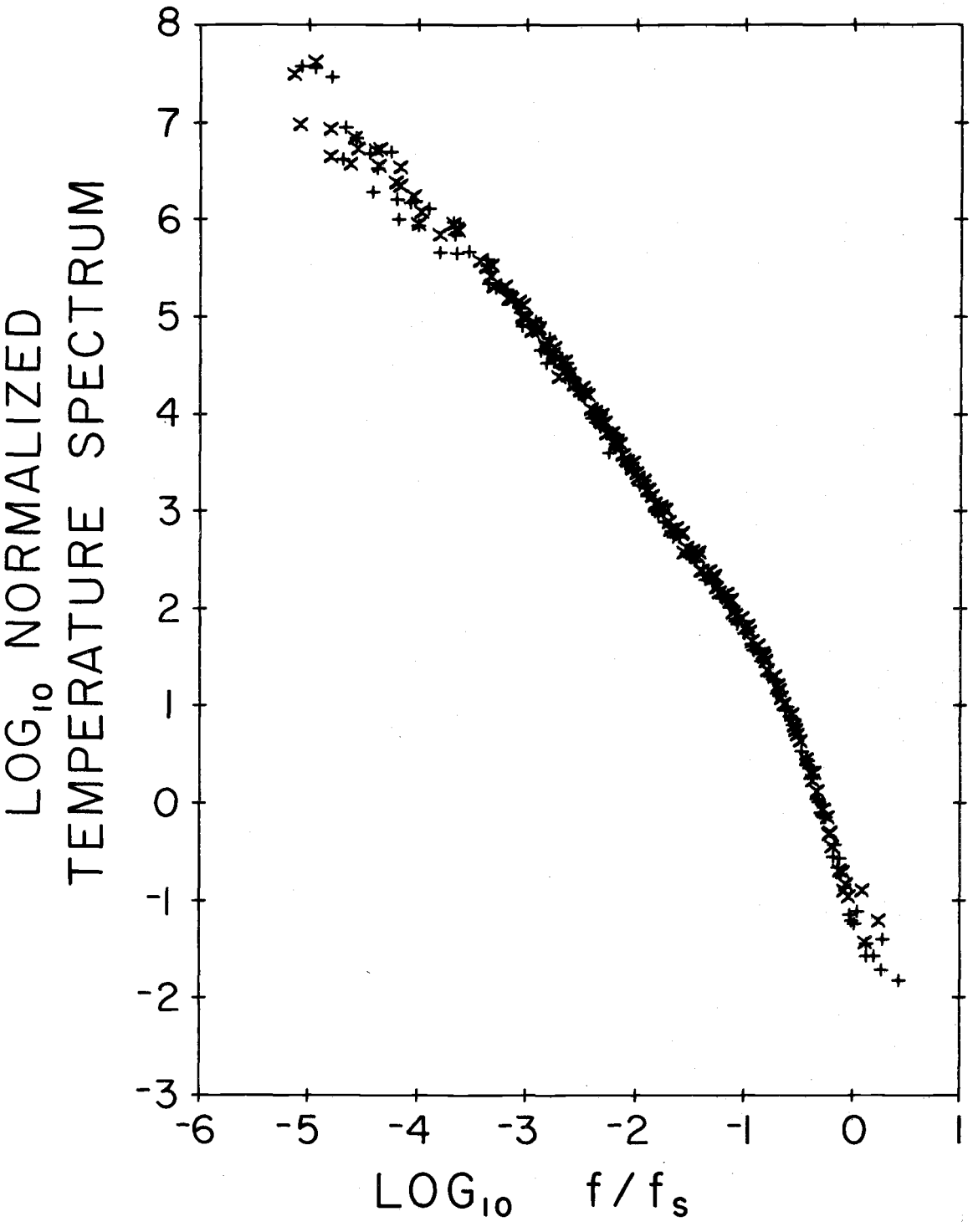

Figure 5-5. Composite Normalized Temperature Spectra.

temperature appears well verified. One discrepancy is the slight slope change at the end of the -5/3 region. This effect is also seen in the temperature derivative spectra and will be further discussed there.

Table 5-3. The one-dimensional Kolmogorov constant for temperature.

Run No.	z/L	ϵ_T ($^\circ C^2$/sec)	β (10 hz)	β (5-28 hz)
RY21C	+.035	.00634	.870	.850
RY22A	-.100	.0920	.954	.970
RY23B	-.078	.137	1.077	1.071
RY24B	-.059	.144	1.130	1.093
RY25C	-.044	.0994	1.183	1.136
RY26B	-.037	.0782	1.152	1.156
RY27A	-.027	.0436	1.061	1.093
B	-.025	.0298	1.059	1.064
RY28A	-.045	.0144	.926	.924
B	-.018	.0031	.988	.974
RY29A	-.006	2.3×10^{-4}	---	---
B	-.006	1.5×10^{-5}	---	---
C	+.023	6.9×10^{-4}	.879	.914
		Average	1.025	1.022
		Standard deviation	.104	.103
		Standard error of mean	.031	.013

The temperature derivative spectra were normalized according to Eqns. (1-16) and (1-20). As with the velocity derivative spectra the temperature derivative spectra may also be referred to as the

temperature dissipation spectra. Figure 5-6 is a plot of the normalized temperature dissipation spectra. There is slightly more variation than in the previous normalized plots, however, at high frequencies the variation is very slight. The unexpected shape as seen in the temperature spectra also appears here as a peaking just before the region of maximum dissipation. This can also be more clearly seen in the spectra of Figure 4-7.

Several possible explanations for this peaking behavior have been examined. These include:

1. local input of thermal variance due to viscous heating
2. electronic resonance
3. velocity sensitivity of the temperature sensor
4. local anisotropy
5. dissimilar dissipation of temperature and velocity fluctuations

The first effect is suggested by Friehe (1973) as a possibly significant source term in the temperature variance budget. The term representing the viscous heating input takes the form of a third-order statistic, $\overline{\theta_v \epsilon}$ since $\epsilon \sim (\frac{\partial u}{\partial x})^2$. To evaluate the magnitude of this term, an estimate was made for θ_v. The temperature fluctuation due to viscous heating can be approximated by conversion of the rate of dissipation, ϵ, into heat as follows:

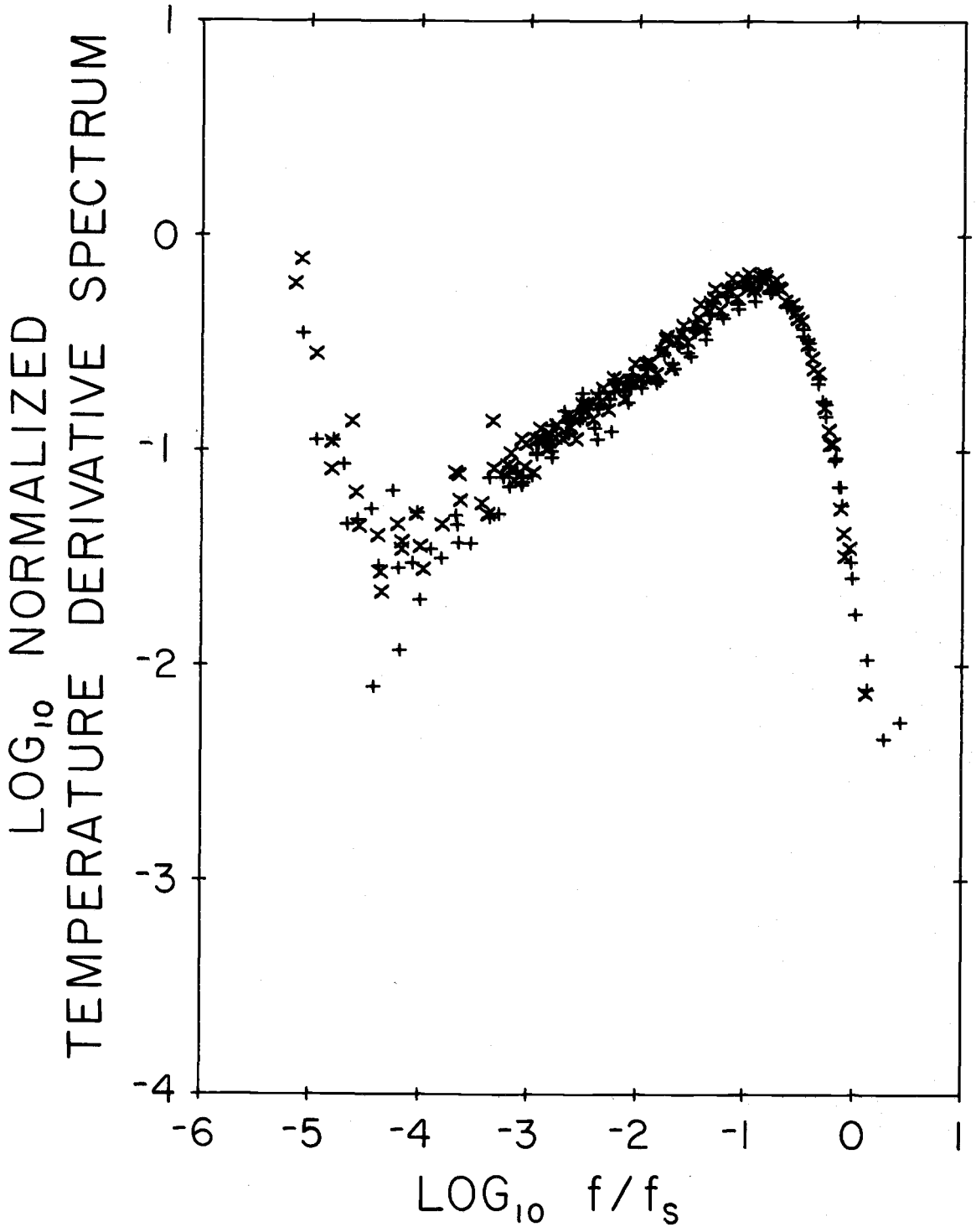

Figure 5-6. Composite Normalized Temperature Derivative Spectra (Temperature Dissipation Spectra).

$$\frac{d\theta}{dt} \approx \frac{\epsilon}{c_p} \tag{5-1}$$

An appropriate time scale is associated with the Kolmogorov micro-scale and is given by:

$$\tau = \frac{1}{f_s} = \frac{2\pi}{\bar{U}} (\nu^3/\epsilon)^{1/4} \tag{5-2}$$

Combining Eqns. (5-1) and (5-2) gives

$$\begin{aligned} \theta_v &\simeq \epsilon\tau/c_p \\ &\simeq \frac{2\pi}{\bar{U}c_p} \nu^{3/4} \epsilon^{3/4} \end{aligned} \tag{5-3}$$

Thus the production term due to viscous heating is approximated by:

$$\overline{\theta_v \epsilon} \simeq \frac{2\pi}{\bar{U}c_p} \nu^{3/4} \epsilon^{7/4} \tag{5-4}$$

An appropriate value for ϵ would not be the mean value but a much larger value associated with the large excursion of the instantaneous ϵ from the mean value. Using the probability distribution of Gibson, et al. (1970) the appropriate value of ϵ is estimated as about $150\ \epsilon_{av}$. Substitution of the values for each run then gives an estimate of the magnitude of the term. For all runs the viscous heating term is more than 5 orders of magnitude smaller than the

thermal dissipation term.

In addition, if this term is significant it should give a greater effect under neutral conditions where the production due to the covariance of $\overline{w\theta}$ is small; however this was not observed. Thus it does not appear that viscous heating is responsible for the observed anomaly in the temperature spectral shape. It would, however, be advisable to measure $\overline{\theta\epsilon}$. This would require a velocity and temperature sensor to be placed within a microscale length of each other (~ 1 mm).

As another possible source of the anomaly, the PRT electronics frequency response was rechecked in the frequencies between 10 hz and 1000 hz to determine the presence of any peaking due to some resonance. The frequency response was found to be flat within less than 1% over this frequency range, thus eliminating this as a possibility.

Wyngaard (1971) discusses the effect of velocity sensitivity of the temperature sensor on temperature spectral measurements. However, for the conditions present for this experiment the spectral effect of velocity sensitivity is on the order of 0.1% and should not be particularly frequency dependent.

Another effect examined was that of local anisotropy in the flow. Examination of the uw cospectra showed that the covariance is negligible after 10 hz. However, the ratio of the vertical velocity

spectrum to that of the horizontal velocity was never near the 4/3 value required for local isotropy. Up to 10 hz the ratio increased but never exceeded 1. It is reasonable to expect that on the very small scales associated with dissipation, conditions would be isotropic. Gibson, et al. (1970) pointed out the possible effects of anisotropy when they demonstrated a nonzero skewness for the temperature derivative. In isotropic flow the derivative skewness is required to be zero. Gibson, et al. postulates that the effect of anisotropy would be to decrease the horizontal temperature gradients while increasing the vertical gradients through the shearing action of the velocity flow by stretching eddies in the horizontal. If this were the case the measured value of $\frac{\partial T}{\partial x}$ would be less than under isotropic conditions, and thus the measured spectral estimates would be lower than expected for frequencies less than the value where local conditions became isotropic. Gibson, et al. used this argument to explain their large values of β since the measured temperature dissipation would be lower under anisotropic conditions (but assuming isotropy) than under isotropic conditions. The possible explanation for the peaking then is that the spectral values near the peak and beyond are closer to the true values than the spectral values at lower frequencies where the effects of anisotropy occur. If this explanation is valid then the measured value of β would be too low by about 20 to 30%. The lower value of β results primarily from the anisotropic effect on the

spectrum and only slightly on the anisotropic effect on the dissipation since this effect occurs at frequencies below the maximum dissipation. Examination of the velocity spectra shows little evidence of a similar effect, however, the peaking is clearly seen in the plot of the Kolmogorov constant for velocity, α (Figure 5-1). Data taken at higher levels such as that of Boston (1970) would presumably have less anisotropy effect, which might explain the lack of peaking in the Boston data.

The final effect examined was that due to dissimilarity between the dissipation of temperature and velocity fluctuations (Schmitz, 1968). Schmitz suggested, in an oral presentation (never published), that the dissipation dissimilarity would result in a slope increase in temperature spectra. It is rather obvious from the strip chart recording (Figure 4-2) that the temperature fluctuations are more intermittent and have different characteristics than the velocity fluctuations. Thus the dissipation of temperature variance is occurring more intermittently and perhaps at different locations in the flow field than the dissipation of turbulent kinetic energy. This dissimilarity could be due to dissimilar production (i.e. dissimilar cospectra, $\overline{uw}$ and $\overline{w\theta}$, and mean vertical gradients). If some of the temperature fluctuations are being dissipated in different spots than the velocity fluctuations they must rely solely on thermal diffusion for dissipation. This would be similar to the situation suggested by

Batchelor (1959) for temperature fluctuations in fluids with large Prandtl numbers where the temperature fluctuations extend to scale sizes much smaller than the velocity fluctuations. Batchelor showed that for scales smaller than the velocity microscale the slope of the temperature spectrum increased to -1 before finally rapidly falling off.

Additional support for this possibility is found when the normalized velocity and temperature dissipation spectra are superimposed. This reveals that the peak of the temperature dissipation is at a higher frequency than the velocity dissipation peak. For fluids with Prandtl number less than 1 (air, Pr = 0.7) the temperature dissipation peak should occur at lower frequencies than the velocity dissipation peak.

C. Flux Comparison

In addition to the high frequency temperature and velocity data simultaneous lower frequency data were obtained and analyzed to obtain direct measures of the momentum and sensible heat fluxes, as outlined in Chapter II. These fluxes were obtained for comparison with the fluxes calculated using the dissipation method also outlined in Chapter II. Table 5-4 gives a summary of the results for all runs. A clearer comparison is seen in Figures 5-7 and 5-8 where the direct results are plotted against the dissipation results. Perfect

Table 5-4. Comparison of fluxes computed by dissipation and direct methods.

Run No.	z/L	τ (dynes/cm^2)	H_s (mw/cm^2)
RY21C	.032	1.28	-5.15
	(+.035)*	(1.02)	(-4.06)
RY22A	-.277	1.04	25.7
	(-.100)	(1.68)	(24.8)
RY23B	-.096	2.46	42.5
	(-.078)	(2.31)	(31.7)
RY24B	-.067	2.64	33.6
	(-.059)	(2.85)	(33.0)
RY25C	-.062	2.51	28.9
	(-.044)	(3.03)	(27.0)
RY26B	-.040	2.99	23.7
	(-.037)	(3.13)	(23.7)
RY27A	-.032	1.93	9.98
	(-.027)	(3.14)	(17.4)
RY27B	-.025	2.67	12.5
	(-.025)	(2.82)	(14.0)
RY28A	-.077	0.93	7.97
	(-.045)	(1.38)	(8.47)
RY28B	-.019	0.88	1.77
	(-.018)	(1.48)	(3.72)
RY29A	-.006	0.93	0.60
	(-.006)	(1.18)	(0.91)
RY29B	-.006	0.94	0.60
	(-.002)	(1.02)	(0.22)
RY29C	+.039	0.42	-1.21
	(+.023)	(0.58)	(-1.18)

*Dissipation values with parenthesis.

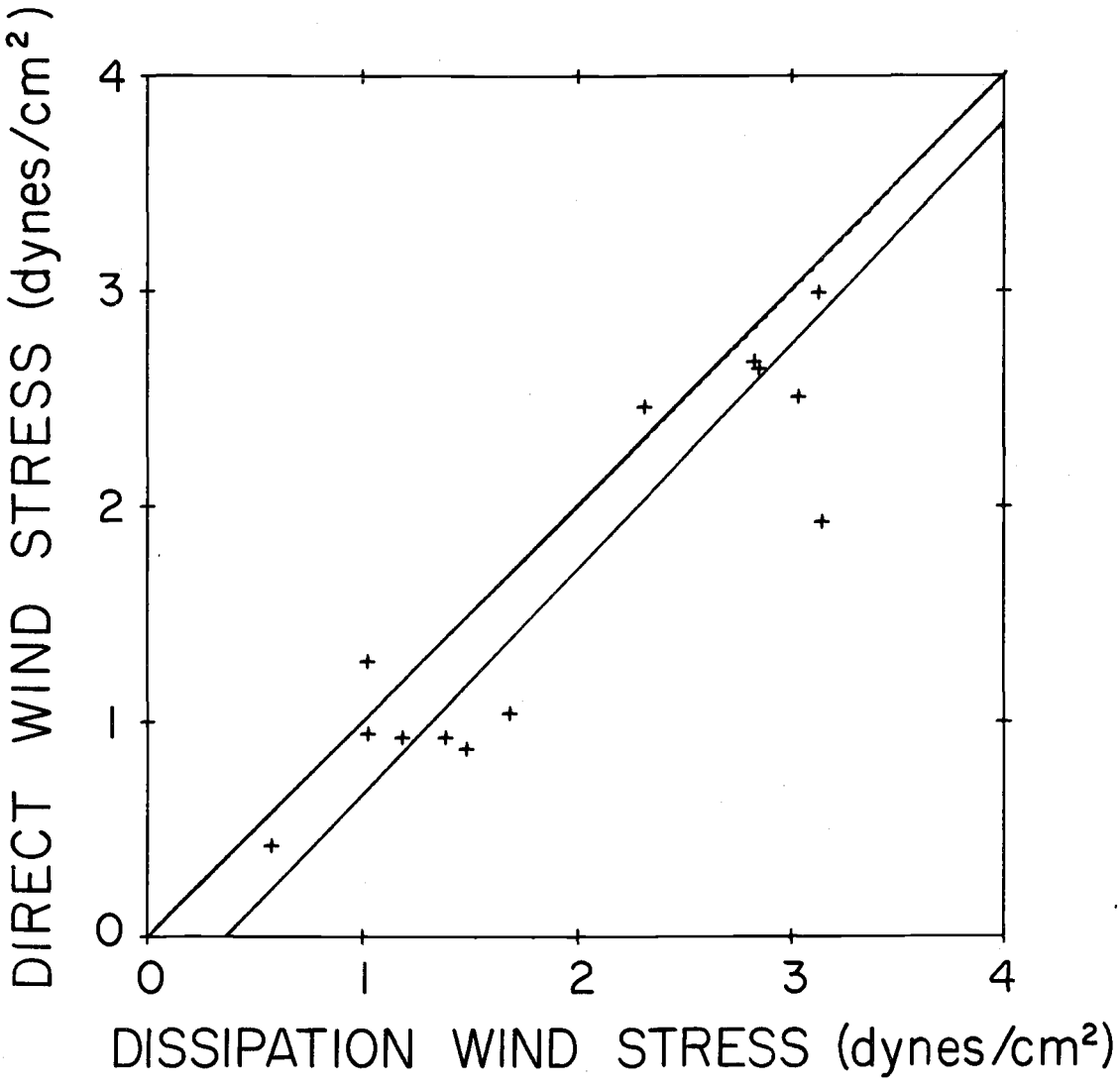

Figure 5-7. Comparison of Momentum Flux Computed by Dissipation and Direct Methods.

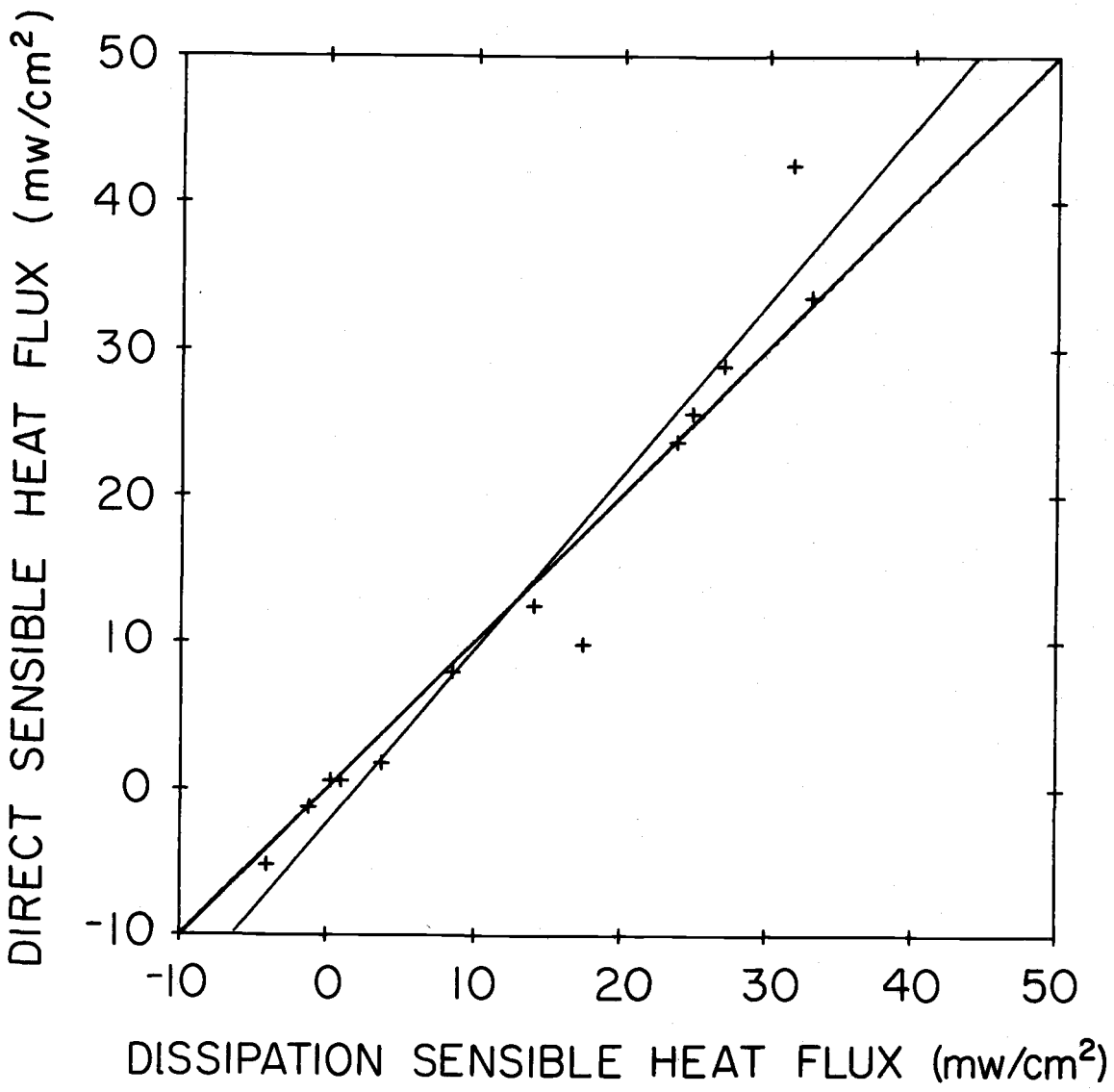

Figure 5-8. Comparison of Sensible Heat Flux Computed by Dissipation and Direct Methods.

agreement would, of course, be a line with slope equal 1. These figures contain the data points, the slope equal 1 line and the linear least-square curve fit to the data. The dissipation method appears to over-estimate the stress by a fixed amount (or the direct method underestimates). Excellent agreement is seen in the sensible heat flux estimates. It might be noted that although the agreement is fairly good the direct method used relatively short records lengths which may not give reliable results since cospectra have low frequency variations. This may in fact explain some of the scatter.

VI. SUMMARY

A. Kolmogorov Universal Constants

The initial primary research objective was to directly determine the one-dimensional Kolmogorov constant for temperature and to remove some of the uncertainty associated with its value. As we have seen, this investigator found the value of the constant to be 1.02 in disagreement with both the indirectly measured values and the recent directly measured values of Boston (1970) and Gibson, et al. (1970). In addition the unexpected anomally in the temperature spectral shape raises additional questions, a common outcome of much research.

The value of the temperature constant is known with perhaps more certainty than before. However, the anomalous behavior of the temperature spectra raises questions about the universality of the constant and its interpretation. Although Boston (1970) suggested a possible stability influence on the constant, for the stability range of this investigation no statistically significant variation was found. However, the questions concerning the effects of anisotropy and dissimilar dissipation have yet to be fully examined.

The value of the one-dimensional Kolmogorov constant for velocity was estimated at 0.50 in good agreement with most other values.

B. Spectral Forms

1. Velocity

The velocity and velocity derivative spectra results agree well with most other results, while extending the spectral measurements to slightly higher frequencies. Normalization of spectra from both stable and unstable conditions results in a simple universal curve which closely agrees with the results of Nasymth (1970).

2. Temperature

Probably the most important contribution of this research is discovery of the anomalous spectral shape for the temperature fluctuations, although conclusive explanations for the anomally was not possible. Most of the possibilities examined can be rejected, while the effects of anisotropy and/or dissimilar dissipation of temperature and velocity fluctuation appear to be the most reasonable possibilities. The result of the peak of the temperature dissipation occurring at a higher frequency than the peak of the velocity dissipation lends further support for the latter hypothesis. It is, therefore, suggested that further investigations involving high frequency temperature fluctuations be made to examine these possibilities and their consequences on the spectral shape and on direct evaluation of the constant, β.

C. Flux Comparison

Based on the comparison of fluxes computed by direct and dissipation methods it is concluded that both techniques are comparable. However, use of the dissipation method requires knowledge of the constant, β, in the inertial subrange spectral form for temperature. As we have seen, the value of the constant is still uncertain.

BIBLIOGRAPHY

Batchelor, G.K. "Small-Scale Variation of Convected Quantities like Temperature in a Turbulent Fluid," J. Fluid Mech., 5, p. 113, 1959.

Boston, N.E.J. "An Investigation of High Wave Number Temperature and Velocity Spectra in Air," Ph.D. Thesis, University of British Columbia, 1970.

Corrsin, S. "On the Spectrum of Isotropic Temperature Fluctuations in an Isotropic Turbulence," J. Appl. Physics, 22, p. 469, 1951.

Flow Corporation Bulletin No. 25. "Hot-wire Anemometry," Flow Corporation, Watertown, Massachusetts, 1956.

Friehe, C.A. "Generation of Temperature Fluctuations by Static Pressure Fluctuations on the Atmospheric Boundary Layer," (to be published).

Gibson, C.H. and W.H. Schwarz. "The Universal Equilibrium Spectra of Turbulent Velocity in Scalar Fields," J. Fluid Mech., 16, p. 365, 1963.

Gibson, C.H., G.R. Stegen and R.B. Williams. "Statistics of the Fine Structure of Turbulent Velocity and Temperature Fields Measured at High Reynolds Number," J. Fluid Mech., 41, p. 153, 1970.

Goldstein, S. Modern Developments in Fluid Dynamics, Oxford Univ. Press, 1938.

Grant, H.L., R.W. Stewart and A. Moilliet. "Turbulence Spectra from a Tidal Channel," J. Fluid Mech., 12, p. 421, 1962.

Grant, H.L., et al. "The Spectrum of Temperature Fluctuations in Turbulent Flow," J. Fluid Mech., 34, p. 423, 1968.

Hinze, J.O. Turbulence, New York, McGraw-Hill, 1959.

Kaimal, J.C., et al. "Spectral Characteristics of Surface-Layer Turbulence," Quart. J. Roy. Met. Soc., 98, p. 563, 1972.

Kolmogorov, A.N. "The Local Structure of Turbulence in Incompressible Viscous Fluids for Very Large Reynolds Numbers," C.R. Acad. Sci. U.R. S.S., 30, p. 301, 1941.

Lumley, J.L. and H.A. Panofsky. The Structure of Atmospheric Turbulence, Wiley, New York, 1964.

McBean, G.A., R.W. Stewart and M. Miyake. "The Turbulent Energy Budget near the Surface," J. Geophys. Res., 76, p. 6540, 1971.

Monin, A.S. and A.M. Obukhov. "Basic Regularity in Turbulent Mixing in the Surface Layer of the Atmosphere," Trudy Geophys. Inst. ANSSR, 24, p. 163, 1954.

Nasmyth, P.W. "Oceanic Turbulence," Ph.D. Thesis, University of British Columbia, 1970.

Obukhov, A.M. "Structure of the Temperature Field in Turbulent Streams," Bull. Acad. Sci. U.S.S.R. Geogr. and Geophys. Ser. 13, p. 58, 1949.

Paquin, J.E. and S. Pond. "The Determination of the Kolmogoroff Constants for Velocity, Temperature and Humidity Fluctuations from Second- and Third-Order Structure Functions," J. Fluid Mech., 50, p. 257, 1971.

Pond, S., R.W. Stewart and R.W. Burling. "Turbulence Spectra in the Wind over Waves," J. Atmos. Sci., 20, p. 319, 1963.

Pond, S., et al. "Spectra of Velocity and Temperature Fluctuations in the Atmospheric Boundary Layer over the Sea," J. Atmos. Sci., 23, p. 376, 1966.

Schmitz, P.D. "Effects of Dissipation Fluctuations on Spectra of Convected Quantities," oral presentation at Symposium on Theoretical Problems in Turbulence Research, The Pennsylvania State University, 1968.

Shieh, C.M., H. Tennekes and J.L. Lumley. "Airborn Measurements of Small-Scale Structure of Atmospheric Turbulence," Phys. Fluids, 14, p. 201, 1971.

Taylor, G.I. "Statistical Theory of Turbulence," Proc. Roy. Soc. (London) A151, p. 421, 1935.

Taylor, G.I. "The Spectrum of Turbulence," Proc. Roy. Soc. (London) A164, p. 476, 1938.

Tennekes, H. and J.L. Lumley. A First Course in Turbulence, The MIT Press, Cambridge, Mass., 1972.

Wyngaard, J.C. "The Effect of Velocity Sensitivity on Temperature Derivative Statistics in Isotropic Turbulence," J. Fluid Mech., 48, p. 763, 1971.

Wyngaard, J.C. and O.R. Coté. "The Budgets of Turbulent Kinetic Energy and Temperature Variance in the Atmospheric Surface Layer," J. Atmos. Sci., 28, p. 190, 1971.